Molecular Biology of the Cell
Vol. 20, 2337–2350, April 15, 2009

Rab11b Regulates the Apical Recycling of the Cystic Fibrosis Transmembrane Conductance Regulator in Polarized Intestinal Epithelial Cells

Mark R. Silvis,* Carol A. Bertrand,* Nadia Ameen,* Franca Golin-Bisello,* Michael B. Butterworth,* Raymond A. Frizzell,*† and Neil A. Bradbury†‡

*Department of Cell Biology and Physiology, University of Pittsburgh School of Medicine, Pittsburgh, PA 15261; and ‡Department of Physiology and Biophysics, Chicago Medical School, Chicago, IL 60064

Submitted January 28, 2008; Revised January 30, 2009; Accepted February 12, 2009
Monitoring Editor: Marcos Gonzalez-Gaitan

The cystic fibrosis transmembrane conductance regulator (CFTR), a cAMP/PKA-activated anion channel, undergoes efficient apical recycling in polarized epithelia. The regulatory mechanisms underlying CFTR recycling are understood poorly, yet this process is required for proper channel copy number at the apical membrane, and it is defective in the common CFTR mutant, ΔF508. Herein, we investigated the function of Rab11 isoforms in regulating CFTR trafficking in T84 cells, a colonic epithelial line that expresses CFTR endogenously. Western blotting of immunoisolated Rab11a or Rab11b vesicles revealed localization of endogenous CFTR within both compartments. CFTR function assays performed on T84 cells expressing the Rab11a or Rab11b GDP-locked S25N mutants demonstrated that only the Rab11b mutant inhibited 80% of the cAMP-activated halide efflux and that only the constitutively active Rab11b-Q70L increased the rate constant for stimulated halide efflux. Similarly, RNAi knockdown of Rab11b, but not Rab11a, reduced by 50% the CFTR-mediated anion conductance response. In polarized T84 monolayers, adenoviral expression of Rab11b-S25N resulted in a 70% inhibition of forskolin-stimulated transepithelial anion secretion and a 50% decrease in apical membrane CFTR as assessed by cell surface biotinylation. Biotin protection assays revealed a robust inhibition of CFTR recycling in polarized T84 cells expressing Rab11b-S25N, demonstrating the selective requirement for the Rab11b isoform. This is the first report detailing apical CFTR recycling in a native expression system and to demonstrate that Rab11b regulates apical recycling in polarized epithelial cells.

INTRODUCTION

Regulation of transport protein copy numbers at the apical and basolateral plasma membranes of polarized epithelial cells controls the vectorial movement of solutes and water and thereby establishes the physiological functions of secretory and absorptive epithelia (Bradbury and Bridges, 1994; Bertrand and Frizzell, 2003). Intestinal epithelia regulate luminal fluidity by balancing solute absorption with regulated salt and water secretion; in the latter process, chloride transport establishes the electrical and osmotic driving forces for secondary sodium and water transport (Barrett and Keely, 2000). The cystic fibrosis transmembrane conductance regulator (CFTR), an apically localized cAMP/protein kinase A (PKA)-activated anion channel, is the primary chloride conductance at the apical membranes of intestinal epithelial cells (Berger *et al.*, 1991; Chan *et al.*, 1992; Cohn *et al.*, 1992; Wagner *et al.*, 1992). Its significance is reflected by the phenotype of CFTR null mice and pigs, which die of intestinal obstruction due to luminal dehydration (Clarke *et al.*, 1994; Rogers *et al.*, 2008). The pathological consequences resulting from the dysregulation or absence of CFTR, as seen in secretory diarrhea or the intestinal obstruction seen in cystic fibrosis, respectively, underscore the critical role of CFTR in intestinal secretory mechanisms.

CFTR-mediated chloride transport is regulated by cAMP/PKA activation of plasma membrane-localized channels as well as by acute modifications in the apical membrane density of CFTR channels in response to agonists (Bertrand and Frizzell, 2003). The latter is accomplished by decreased internalization of CFTR channels from the plasma membrane and increased exocytic insertion of additional CFTR from intracellular pools. Morphological studies examining CFTR localization in native tissue and polarized epithelial cells have noted both apical plasma membrane- and subapical intracellular-localized CFTR populations (Zeitlin *et al.*, 1992; Prince *et al.*, 1993; Bradbury *et al.*, 1994; Webster *et al.*, 1994; Ameen *et al.*, 2000). However, few studies have investigated the identity of the CFTR-containing, subapical compartments that are responsible for acute modifications in apical membrane copy number, especially in a polarized epithelium that expresses CFTR endogenously.

In the absence of agonist, CFTR channels in the apical membrane are not static. Rather, CFTR undergoes rapid, constitutive endocytosis (Prince *et al.*, 1994) via clathrin-coated vesicles (Bradbury *et al.*, 1994; Prince *et al.*, 1994;

This article was published online ahead of print in *MBC in Press* (http://www.molbiolcell.org/cgi/doi/10.1091/mbc.E08–01–0084) on February 25, 2009.

†Co-senior authors.

Address correspondence to: Raymond A. Frizzell (frizzell@pitt.edu).

Abbreviations used: ARE, apical recycling endosome; cAMP, cyclic adenosine monophosphate; CFTR, cystic fibrosis transmembrane conductance regulator; EM, electron microscopy; EGFP, enhanced green fluorescent protein; PKA, protein kinase A; TER, transepithelial resistance; Isc, short circuit current.

© 2009 by The American Society for Cell Biology

Varga *et al.*, 2004) through interactions with the AP-2 adaptor complex (Weixel and Bradbury, 2000) and in concert with the actin motor, myosin VI (Swiatecka-Urban *et al.*, 2004; Ameen and Apodaca, 2007). With a half-life of more than 20 h in native expression systems (Varga *et al.*, 2004), the majority of internalized CFTR channels are not degraded, but rather undergo efficient recycling back to the apical plasma membrane (Prince *et al.*, 1994), otherwise channel copy number at the membrane would be depleted. Indeed, work by Swiatecka-Urban *et al.* (2007) demonstrates that CFTR recycling in polarized CFBE41o- cells, a bronchial epithelial cell line transduced to express wild-type CFTR exogenously, requires Myosin Vb. However, the mechanisms that regulate the efficient recycling of CFTR and its importance in modulating apical membrane CFTR copy number remain poorly understood, particularly for native expression systems.

Members of the Rab family of small GTPases localize to specific subcellular compartments of eukaryotic cells where they regulate membrane trafficking processes, including budding, targeting, docking, and fusion of vesicles (Zerial and McBride, 2001; Deneka *et al.*, 2003). GTP binding allows Rab proteins to engage effectors that mediate downstream trafficking events, whereas GTP hydrolysis by their intrinsic GTPase activity inactivates Rabs and halts vesicular traffic. The Rab11 subfamily of Rab GTPases, including Rab11a and Rab11b, has been implicated in membrane recycling in polarized epithelial models (Goldenring *et al.*, 1994, 1996). Rab11a is expressed ubiquitously (Sakurada *et al.*, 1991), whereas Rab11b is enriched in brain, heart, and testis (Lai *et al.*, 1994). The Rab11a and Rab11b isoforms share 89% amino acid homology, with the least similarity found in their membrane-binding hypervariable C-termini (Lai *et al.*, 1994).

Rab11a localizes to the pericentriolar, microtubule-associated apical recycling endosome (ARE) in polarized epithelial cells (Casanova *et al.*, 1999; Leung *et al.*, 2000). It regulates the apical recycling and exocytic insertion of numerous membrane proteins, including the polymeric immunoglobulin receptor (pIgR) in Madin-Darby canine kidney (MDCK) cells (Casanova *et al.*, 1999; Wang *et al.*, 2000), the bile salt export pump (ABCB11) in hepatic cells (Wakabayashi *et al.*, 2004), and the H^+,K^+-ATPase in gastric parietal cells (Duman *et al.*, 1999). In addition, a role for Rab11a has been implicated in the recycling of exogenously expressed CFTR in polarized airway cells (Swiatecka-Urban *et al.*, 2005).

Less is known about Rab11b, which localizes to apical vesicles disparate from the Rab11a-labeled compartment in the pericentriolar region of polarized MDCK and gastric parietal cells (Lapierre *et al.*, 2003). In nonpolarized cells, Rab11b controls transferrin receptor recycling (Schlierf *et al.*, 2000) and Ca^{2+}-induced exocytosis of human growth hormone (Khvotchev *et al.*, 2003). However, there are no data supporting a role for Rab11b in apical recycling in polarized epithelial cells.

Herein, we examined the functions of Rab11a and Rab11b in regulating apical CFTR trafficking in a physiologically relevant system that expresses CFTR endogenously and recapitulates the salt secretion functions of the large intestinal epithelium. Our data suggest that although CFTR localizes to both Rab11a and Rab11b compartments, only Rab11b functions to regulate CFTR recycling to the apical plasma membrane.

MATERIALS AND METHODS

Cell Culture, Electroporation, and Adenoviral Transduction

T84 cells (ATCC, Manassas, VA) were grown in DMEM/F12 (Invitrogen, Carlsbad, CA) supplemented with 5% FBS (Hyclone, Logan, UT) and maintained at 37°C in a humidified atmosphere of 5% CO_2. Cells were passaged weekly when they neared confluency. Cells were seeded onto 6.5-mm transwell filters (Costar, Acton, MA) for immunofluorescence and Ussing chamber experiments or onto 24-mm transwell filters for cell surface biotinylation and apical recycling assays. Seeded cells were fed the next day and then every other day thereafter and grown for 5–10 d until they developed a transepithelial resistance (TER) of >2000 Ω cm^2.

For SPQ [6-methoxy-*N*-(3-sulfopropyl) quinolinium] assays, electroporation of T84 cells was performed with Amaxa's Nucleofector II according to the manufacturer's instructions (Amaxa, Gaithersburg, MD). Briefly, electroporations were performed with 2 μg, (for green fluorescent protein [GFP]-fused Rab11a or Rab11b constructs) or 20 μg (for GFP-tagged short hairpin RNA [shRNA] constructs) DNA per 2×10^6 cells in Solution T and with Nucleofector II program, W017. Electroporated cells were seeded onto poly-L-lysine (Sigma-Aldrich, St. Louis, MO)-coated 25-mm glass coverslips (Fisher Scientific, Pittsburgh, PA) in a solution of Opti-MEM (Invitrogen)–DMEM/F12 T84 media (1:1). The Opti-MEM/DMEM-F12 was replaced with normal T84 media at 16 h after electroporation, and cells were then fed every other day and used for SPQ fluorescence experiments 3–5 d later (for GFP-fused Rab11a or Rab11b constructs) or 5–7 d later (for GFP-tagged shRNA constructs). Visual inspection of the GFP-expressing cells relative to nonexpressing cells revealed an electroporation efficiency of ~75% at 24 h after electroporation. Loss of GFP expression was observed as early as 48 h after electroporation.

Adenoviral transductions of T84 cells were performed as described previously (Hallows *et al.*, 2003). Briefly, 5–7-d-old filter-grown T84 monolayers were washed four times with 37°C PBS lacking $CaCl_2$ and $MgCl_2$ (PBS−CM) to disrupt the tight junctions. The filters were removed from the plates, placed in a 10 cm^2 dish on drops of PBS −CM (20 μl basolateral and 40 μl apical for 6.5-mm filters or 100 μl basolateral and 300 μL apical for 24-mm filters) containing recombinant adenovirus at an MOI of 100. Filters were maintained at 37°C in a humidified atmosphere of 5% CO_2 for 1 h in the presence of adenovirus. Ten milliliters of media was then added to the 10-cm^2 dish (basolateral compartment), and cells were allowed to recover until the next day when normal media were added to the apical and basolateral sides. The monolayers were used when the TER had recovered fully, within 48 h of infection for Ussing chamber experiments or 24 h after infection for apical plasma membrane biotinylation and recycling assays.

Antibodies

All antibodies were used at 1:1000 for immunofluorescence (IF) and Western blotting unless otherwise stated. Mouse monoclonal antibodies for IF detection of CFTR were obtained from Millipore (M3A7, Billerica, MA) or purified from the mouse hybridoma clone 24–1 (ATCC) via ammonium sulfate precipitation, and each was used at 1:500. The CFTR monoclonal 596 antibody (Cystic Fibrosis Folding Consortium) was used at 1:5000 for blotting of CFTR. The CFTR antibody used to stain rat tissue was produced and described previously (Ameen *et al.*, 1995). The rabbit polyclonal Rab11a antibody was obtained from Invitrogen and used at 1:500 for Western blotting. The rabbit polyclonal Rab11b antibody used for IF (1:500) was kindly provided by Dr. J. Goldenring (Vanderbilt University, Nashville, TN) and was described previously (Lapierre *et al.*, 2003). The rabbit polyclonal Rab11b antibody from Cell Signaling (Danvers, MA) was used for Western blotting. The rabbit polyclonal zona occludin-1 (ZO-1) antibody was obtained from Invitrogen. The Rab21 polyclonal antibody (1:500 for IF) was kindly provided by Dr. Jack A. M. Fransen (University of Nijmegen, The Netherlands) and was described previously (Opdam *et al.*, 2000). The polyclonal Rab11a (Invitrogen), Rab11b (Cell Signaling), and Rab21 antibodies were used for immunoisolations. Mouse monoclonal pan-Rab11 and Bip/GRP78 antibodies were from BD Transduction Laboratories (San Jose, CA). Goat anti-mouse-FITC and goat anti-Rabbit-Cy3 were obtained from Jackson ImmunoResearch Laboratories (West Grove, PA) and used to label primary antibodies in IF experiments.

DNA Constructs, RT-PCR, and Rab11a– and Rab11b–S25N Adenoviruses

GFP-tagged Rab11a S25N and Q70L constructs were obtained from Dr. M. Zerial (Max Planck Institute, Dresden, Germany). For RT-PCR analysis, T84 cell cDNA was generated with reverse transcriptase and oligo dT primers from mRNA isolated from polarized cells using the Purelink Micro-to-Midi RNA isolation kit from Invitrogen. The full-length human Rab11a and Rab11b transcripts were amplified from T84 cDNA using the following primers: Rab11a: forward, ATG GGC ACC CGC GAC GAC; reverse, TTA GAT GTT CTG ACA GCA CTG CAC C; and Rab11b: forward, GGG GAC CCG GGA CGA CGA GTA C; and reverse, CAC AGG TTC TGG CAG CAC TGC AGC. Amplicons were separated on an agarose gel containing ethidium bromide to examine the presence of the Rab11 isoform transcripts. Amplified human Rab11a and Rab11b were TOPO cloned into the pCR2.1 vector (Invitrogen) and then sequenced using M13 primers (Invitrogen). Results were verified by BLAST search, and Rab11b was subcloned into pEGFP-C1 (Invitrogen) using NheI and XhoI sites (New England Biolabs, Ipswich, MA). The S25N and Q70L point mutations were introduced into the wild-type GFP-Rab11b construct using the Quick-Change Site-directed Mutagenesis kit (Qiagen, Valencia, CA) following the manufacturer's instructions. The following primers

were used: S25N, forward primer, GGC GTG GGC AAG AAC AAC CTG CTG TCG; and Q70L: forward primer, GAC ACC GCT GGC CTG GAG CGC TAC CGC. All constructs were sequenced before use.

Recombinant adenovirus expressing GFP-tagged Rab11a-S25N (pAdTet-GFP-Rab11aS25N) was kindly provided by Dr. Asli Oztan (University of Pittsburgh, PA). Recombinant adenovirus expressing GFP-Rab11b-S25N was created using the ViraPower Adenoviral Expression System from Invitrogen according to the manufacturer's instructions. Briefly, GFP-tagged Rab11b-S25N was amplified using the following primers (forward, CAC CTT GGT ACC GGT CGC CAC CAT GGT GAG CAA GGG; reverse, TTG CGG CCG CGC TGA TTA TGA TCA GTT ATC TAG ATC CGG); TOPO cloned into the Gateway pENTR/D-TOPO vector and then recombined into the pAd/CMV/V5-DEST vector using LR Recombinase. 293A cells were transfected with pAd/CMV/V5-DEST-GFP-Rab11b-S25N using Lipofectamine 2000 (Invitrogen). High-titer adenovirus stocks were purified from 293A crude cell homogenates using the Vivapure AdenoPACK 100 kit (Sartorius, Edgewood, NJ) by following the manufacturer's instructions.

SureSilencing shRNA plasmids containing GFP-tagged shRNAs for Rab11a- or Rab11b- specific knockdown were obtained from SABiosciences (Frederick, MD).

Immunoisolation of Rab11-positive Endosomes

An endosome-enriched fraction containing vesicles positive for markers of the early and recycling endosomal populations was obtained using a modified protocol (Trischler *et al.*, 1999) from that described originally (Gorvel *et al.*, 1991). Briefly, T84 cells were washed twice with PBS at 4°C and scraped in 300 μl homogenization buffer (3 mM imidazole, pH 7.4, 250 mM sucrose, 0.5 mM EDTA, and Complete EDTA-free Protease Inhibitor cocktail; Roche Diagnostics, Indianapolis, IN). Cells were homogenized by 20 strokes of a tight fitting Dounce homogenizer and then centrifuged for 10 min at 3000 rpm in a table-top centrifuge. The resulting postnuclear supernatant (PNS) was adjusted to 40.6% sucrose using 62% sucrose. The diluted PNS was placed in 12-ml capacity Polyclear centrifuge tubes (Sorvall, Newtown, CT) and overlayed with 6 ml of 35% sucrose and 4 ml of 25% sucrose and then centrifuged in a TH-641 rotor at 108,000 $\times$ *g* for 3 h at 4°C. The endosome-enriched fraction at the 25%/35% sucrose interface was collected (approximately 1 ml), diluted threefold with PBS and spun at 108,000 $\times$ *g* for 30 min at 4°C. Pelleted endosomes were resuspended in 1 ml of 0.1% BSA/PBS per variable. Rabbit anti-Rab11a, anti-Rab11b, anti-Rab21, or a nonspecific rabbit IgG were added and incubated with the isolated endosomes overnight at 4°C with rotation. In addition, 50 μl sheep anti-rabbit magnetic Dynabeads (Invitrogen; per variable) were washed with 1% BSA/PBS three times and incubated with 1 ml 1% BSA/PBS overnight at 4°C. The following day the beads were recovered with a magnet and resuspended in 50 μl of 1% BSA/PBS per variable. Fifty microliters of the blocked and washed beads were then added and incubated with each of the antibody–endosome fractions for 6 h at 4°C with rotation. The bead–antibody–endosome complexes were collected with a magnet and washed twice with 1% BSA/PBS, once with 0.1% BSA/PBS, and then once with PBS. Laemmli sample buffer was added to the immunoisolated endosomes, and samples were resolved by 10% SDS-PAGE, transferred to PVDF, and then blotted for proteins of interest.

Immunofluorescence Labeling

All steps were performed at 4°C unless stated otherwise. Polarized, filter-grown T84 cells were rinsed twice with PBS containing 0.1 mM $CaCl_2$ and 1 mM $MgCl_2$ (PBS+CM) and 5 mM DTT and then incubated with gentle shaking for 10 min in the second wash. Cells were then rinsed gently with PBS+CM six times to remove surface-accumulated mucus. Cells were fixed with 5% paraformaldehyde in PBS+CM for 30 min and then permeabilized with 0.1% Triton X-100 in PBS+CM for 10 min. Cells were labeled in blocking buffer consisting of 10% goat serum, 10% dry nonfat milk, 10 mg/ml BSA, and 0.05% Triton X-100 in PBS+CM overnight at 4°C with gentle shaking. Unbound primary antibody was removed by four washes with PBS+CM. Primary antibodies were labeled with corresponding fluorescence-conjugated secondary antibodies in blocking buffer for 2 h. Cells were washed again, then mounted on coverslips, and used for confocal microscopy.

Cryostat sectioning and indirect immunofluorescence performed on rat jejunum was performed as described previously (Ameen and Apodaca, 2007).

Rat jejunum enterocytes were isolated as described previously (Ameen *et al.*, 2003). An endosome-enriched fraction used for immunogold electron microscopy (EM) was obtained from homogenized rat enterocytes as described above for T84 cells. Endosomes from the 25%/35% sucrose interface were washed in 0.1 M phosphate buffer, pH 7.4, and fixed in 2% paraformaldehyde for 1 h, and endosomes were immunolabeled to detect CFTR (15-nm gold) and Rab11 (5-nm gold) as described previously (Ameen *et al.*, 2000).

SPQ Fluorescence Assays

SPQ halide efflux assays were performed on electroporated T84 cells as described previously (Chao *et al.*, 1989; Yang *et al.*, 1993; Howard *et al.*, 1995). Briefly, the iodide-sensitive fluorescent indicator, SPQ (Molecular Probes, Eugene, OR) was introduced into T84 cells in a hypotonic solution of iodide buffer (in mM: 130 NaI, 4 KNO_3, 1 $Ca(NO_3)_2$, 1 $Mg(NO_3)_2$, 10 glucose, and 20 HEPES, pH 7.4) diluted 1:1 with water and containing a final concentration of 10 mM SPQ. Cells were loaded for 20 min at 37°C in a humidified chamber with 5% CO_2. The SPQ-loaded cells were then mounted on a Nikon Diaphot 300 inverted microscope (Melville, NY) with a 37°C heated stage and perfused with iodide buffer while regions of interest (ROIs) were for chosen for GFP and non-GFP–expressing cells using the Simple PCI Version 5.1 software (Compix Imaging Systems, Cranberry Township, PA). The GFP signal intensity varied from cell to cell; therefore, three cell populations were chosen (based on GFP expression levels as estimated by visual inspection of the cells) for SPQ fluorescence data collection (see Supplemental Figure S2). Changes in CFTR-mediated SPQ fluorescence were monitored at the 445-nm wavelength in response to excitation at 340 nm during perfusion at 37°C in nitrate buffer (NaI replaced with 130 mM $NaNO_3$) for 3 min without forskolin and then for 8 min with 10 μM forskolin added. The slopes or single-exponential rates were calculated using SigmaPlot Version 7.1 for each mean fluorescence trace generated from the >50 cells examined per population per coverslip.

Ussing Chamber Experiments

T84 cells cultured on transwell filters were mounted in modified Costar Ussing chambers, and the cultures were short circuited continuously with an automatic voltage clamp to record the transepithelial short circuit current (Isc) as described previously (Butterworth *et al.*, 2005). The bathing Ringer's solution was composed of (in mM) 120 NaCl, 25 $NaHCO_3$, 3.3 KH_2PO_4, 0.8 K_2HPO_4, 1.2 $MgCl_2$, 1.2 $CaCl_2$, and 10 glucose. The chambers were continuously gassed with a mixture of 95% O_2, 5% CO_2 at 37°C, which maintained the pH at 7.4. Stocks of forskolin (10 mM in 100% ethanol) and bumetanide (20 mM in DMSO) were both used at 1:1000 dilution into the bath.

Cell Surface Biotinylation and Apical Recycling Assays

Cell surface biotinylation and apical recycling assays were performed as described previously (Elferink and Strick, 2005). Briefly, biotinylation of polarized T84 monolayers for the quantitation of apical cell surface CFTR protein levels was performed with the EZ-Link Sulfo-NHS-LC-LC-Biotin (Pierce, Rockford, IL), whereas biotin protection assays to measure recycling required the use of the disulfide-cleavable, EZ-Link Sulfo-NHS-SS-Biotin (Pierce). Experiments were performed in a cold room on ice with all solutions at 4°C unless otherwise stated. To biotinylate apical membrane proteins, adenovirus-transduced, polarized T84 monolayers were rinsed once with PBS+CM and then incubated with PBS+CM containing 5 mM DTT (Sigma) for two 10-min periods with gentle rocking to remove the accumulated surface mucus. After three 10-min PBS+CM washes to remove all excess PBS+CM/DTT, PBS+CM containing 10% FBS was added to the basolateral surface. The apical surface was biotinylated with 1 mg/ml EZ-Link Sulfo-NHS-LC-LC-Biotin (or EZ-Link Sulfo-NHS-SS-Biotin for recycling assays) in borate buffer (85 mM NaCl, 4 mM KCl, and 15 mM $Na_2B_4O_7$, pH 9) for 30 min with gentle agitation. Excess biotin was removed with two 10-min washes in PBS+CM/10% FBS followed by two washes in PBS+CM.

For cell surface CFTR quantitation, cells were lysed in 700 μl biotinylation lysis buffer (BLB; 0.4% deoxycholate, 1% NP40, 50 mM EGTA, 10 mM Tris-Cl, pH 7.4, and Complete EDTA-free Protease Inhibitor Cocktail; Roche Diagnostics). Total protein levels were determined, and normalized samples were incubated overnight with 150 μl UltraLink Immobilized NeutrAvidin Protein Plus (Pierce). Precipitated proteins were washed three times with BLB, solubilized with Laemmli sample buffer, separated on a 10% SDS-PAGE and blotted for CFTR.

For apical recycling assays, the biotinylated membrane proteins were internalized during a 20-min incubation in T84 media at 37°C (two filters were kept at 4°C for the cell surface labeling and stripping controls). Proteins remaining at the cell surface after 20 min at 37°C were stripped of biotin with four 15-min washes in MESNA (Sodium 2-mercaptoethane-sulfonate) stripping buffer (50 mM MESNA, 150 mM NaCl, 1 mM EDTA, 0.2% BSA, and 20 mM Tris, pH 8.6). To detect the recycling of internalized, biotinylated proteins, three filters were quickly warmed to 37°C with T84 media containing 10 μM forskolin for 1, 2.5, or 7.5 min and then immediately cooled to 4°C. Biotinylated proteins that recycled to the cell surface were then stripped of biotin with four 15-min MESNA washes followed by cell lysis and processing as described above.

Statistical Analysis

Statistical significance was determined using Student's *t* test. $p < 0.05$ was considered significant.

RESULTS

Endogenous CFTR Localizes to Punctate Vesicles at the Apical Pole of Polarized T84 Cells

The colonic epithelial cell line, T84, forms polarized monolayers that are similar both morphologically and functionally to intact intestinal tissues and therefore serve

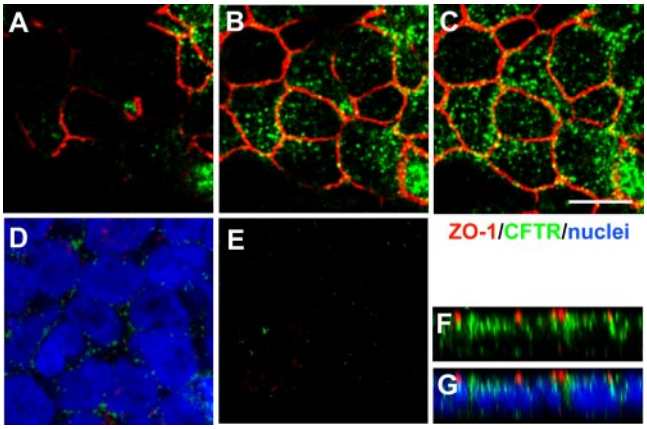

Figure 1. Localization of endogenous CFTR in polarized T84 cells. (A–G) T84 cells were grown on transwell supports for 7–10 d and then fixed and immunostained for ZO-1 (red), CFTR (green), and nuclei (blue) as described in *Materials and Methods.* Confocal cross sections were taken at 1 μm (A), 2 μm (B), 3 μm (C), 6 μm (D), and 12 μm (E) from the first apically detectable fluorescence. (F) The XZ section demonstrates localization of endogenous CFTR (green) within apposition and subapical to the apical tight junction protein, ZO-1 (red). The identical XZ section is shown with nuclei (G). Scale bar, 5 μm.

as a relevant model for studying the contribution of polarized protein trafficking to vectorial electrolyte transport (Dharmsathaphorn *et al.*, 1984; Mandel *et al.*, 1986; Chao *et al.*, 1989). T84 cells express CFTR endogenously (Cohn *et al.*, 1992; Zeitlin *et al.*, 1992) and have been used extensively to characterize CFTR-mediated chloride secretion (Bell and Quinton, 1992; Barrett, 1993). We examined CFTR cellular localization in this system by performing confocal microscopy using indirect immunofluorescence. CFTR localized to punctate, vesicle-like structures at the apical pole of polarized T84 cells (Figure 1, A–E) that were at and beneath the apical plasma membrane as determined by their juxtaposition with the tight junction marker, ZO-1. Analysis of confocal stacks in the XZ plane (Figure 1, F and G) confirmed that CFTR localized to the apical membrane domain in this system. Our findings are in agreement with prior studies of the polarized localization of endogenous CFTR in epithelia, including T84 cells (Cohn *et al.*, 1992; Denning *et al.*, 1992; Tousson *et al.*, 1996).

CFTR Colocalizes with Both Rab11a and Rab11b in Polarized T84 Cells

Several studies have suggested that CFTR found within the subapical vesicle population in native systems is localized to endocytic and recycling compartments that facilitate its apical membrane trafficking (Bradbury *et al.*, 1994; Webster *et al.*, 1994; Ameen *et al.*, 2000). Indeed, efficient CFTR endocytosis and recycling have been demonstrated in T84 cells (Prince *et al.*, 1994); however, no studies have examined the localization of CFTR relative to known markers of membrane recycling compartments in this system. Given the role of Rab11 in regulating the recycling of membrane proteins (Leung *et al.*, 2000; Wang *et al.*, 2000), we speculated that CFTR would be present within the Rab11 recycling compartment. To test this, we first examined the expression of the Rab11a and Rab11b isoforms in T84 cells. Figure 2A reveals the presence of both Rab11a and Rab11b transcripts (lanes 1 and 3) as detected by RT-PCR using isoform-specific primers on cDNA generated from polarized T84 cell mRNA. Western blotting of cell lysates using Rab11a- or Rab11b-specific antibodies identified single bands of the expected 25-kDa molecular weight, confirming the expression of both isoforms in this system (Figure 2B).

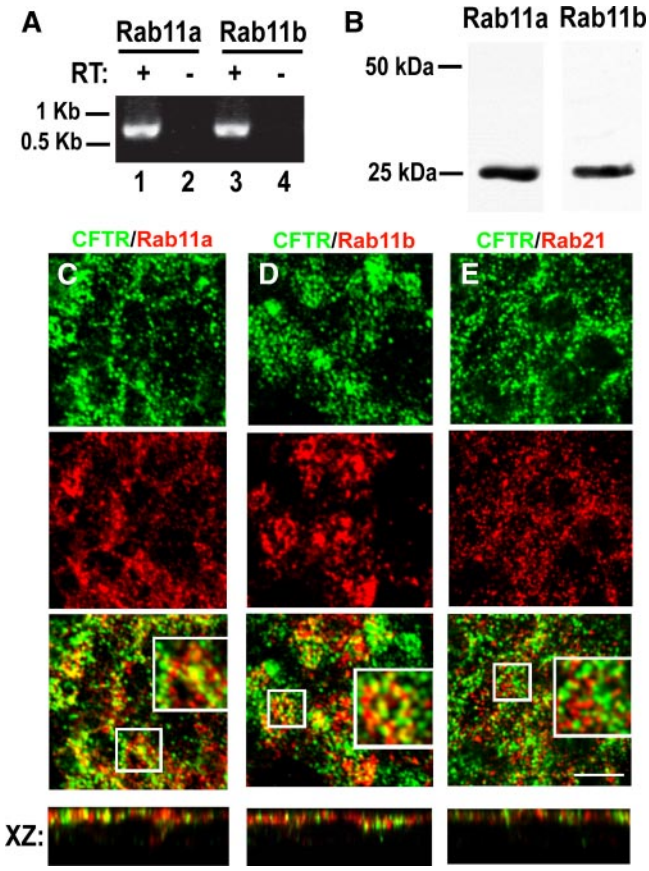

Figure 2. Rab11a and Rab11b are expressed in T84 cells and colocalize with CFTR. (A and B) Expression of the Rab11 isoforms in T84 cells. (A) RT-PCR using Rab11a- or Rab11b-specific primers was performed using mRNA isolated from polarized T84 cells. Reactions without reverse transcriptase (RT) in lanes 2 and 4 confirm the absence of a genomic DNA contribution to the products from the mRNA samples. (B) Western blot analysis of T84 cell lysates with Rab11a- or Rab11b-specific antibodies shows the presence of each Rab11 isoform at the expected molecular weight of 25 kDa. (C–E) Endogenous CFTR colocalizes with Rab11a and Rab11b at the apical pole in T84 cells. Confocal microscopic sections of polarized T84 cells stained for CFTR (green) and Rab11a (C), Rab11b (D), or Rab21 (E; red). Both Rab11a and Rab11b colocalize with CFTR at the apical domain (yellow, bottom panel and XZ). Insets show enlarged regions within white boxes. Confocal sections shown were obtained at 3 μm below the first detectable fluorescence at the apical surface (see Figure 1C). Scale bar, 5 μm.

We next examined whether CFTR colocalized with either Rab11a or Rab11b by immunostaining polarized T84 monolayers. Confocal microscopy revealed that Rab11a localized to the apical pole of T84 cells (Figure 2C, XZ) with a staining pattern that was more diffuse than the pericentriolar localization of Rab11a originally reported in MDCK cells (Casanova *et al.*, 1999). CFTR staining overlapped significantly with that of Rab11a (Figure 2C, bottom panel and XZ), demonstrating that CFTR in T84 epithelia localizes to the ARE as defined by the presence of Rab11a in MDCK cells (Leung *et al.*, 2000). Next, we examined CFTR localization in relation to Rab11b, shown previously to localize to a different internal compartment than the Rab11a-identified ARE in

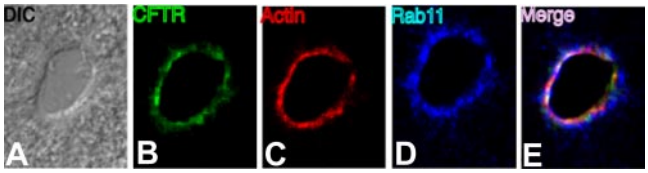

Figure 3. CFTR and Rab11 colocalize in rat intestinal crypts in vivo. (A–E) Cryostat sections through rat jejunum at the level of the crypt are displayed. (A) Differential interference contrast (DIC) image showing histology of the section stained for CFTR (B), actin (C), and Rab11 (D). (E) Merge demonstrates that CFTR colocalizes with Rab11 and actin at the apical pole of the crypt-lining enterocytes.

MDCK cells (Lapierre *et al.*, 2003). Rab11b displayed a staining pattern at the apical pole of T84 cells similar to that reported previously for MDCK cells, and it also overlapped significantly with endogenous CFTR (Figure 2D, bottom panel and XZ). Finally, we also examined CFTR localization in relation to Rab21. Rab21 was identified and characterized in intestinal epithelial Caco-2 cells where it colocalizes with known markers of the early endocytic pathway at the apical membrane (Opdam *et al.*, 2000; Simpson *et al.*, 2004). Rab21 staining was more punctate than the staining observed for either Rab11a or Rab11b. We observed minor colocalization of CFTR with Rab21 compared with Rab11a or Rab11b (Figure 2E), which suggests that CFTR is not localized primarily to this apical endocytic compartment under steady-state conditions. We conclude that endogenous CFTR localizes to both the Rab11a-identified ARE and Rab11b-positive compartments in polarized intestinal epithelial cells.

CFTR and Rab11 Colocalize In Vivo

Cryo-immunogold EM on rat intestine has demonstrated CFTR localization to the apical plasma membrane and within subapical vesicles of enterocytes lining the crypt (Ameen *et al.*, 1999; Ameen *et al.*, 2000). Early studies examining Rab11 localization in rabbit epithelial tissues, including the intestine, revealed prominent vesicular-like staining in the apical region (Goldenring *et al.*, 1996). To examine whether CFTR colocalized with Rab11 in native tissue, we costained isolated cryostat sections of rat jejunum with CFTR, Rab11, and actin antibodies and analyzed their localization by confocal microscopy (Figure 3, A–E). The Rab11 antibody used for this experiment recognizes both Rab11a and Rab11b (*Materials and Methods*). We observed that CFTR colocalized with Rab11 and actin in native tissue at the apical region of enterocytes lining the crypt. We were unable to examine isoform-specific colocalization with CFTR in vivo because of the unavailability of isoform specific antibodies that recognize rat tissue. We conclude that CFTR is localized to apical, Rab11-positive recycling endosomes in rat intestine.

Immunomagnetic Isolation of Rab11-positive Vesicles Reveals the Presence of CFTR

Studies examining the role of Rab GTPases in membrane trafficking have utilized immunoisolation of Rab-positive vesicles from endosome-enriched subcellular fractions (Gorvel *et al.*, 1991; Trischler *et al.*, 1999). This biochemical technique allows for the isolation of intact, specific Rab-bearing compartments with subsequent identification of associated proteins. Although our immunofluorescence data suggests that CFTR colocalizes with both Rab11a and Rab11b, it does not necessarily place CFTR within the Rab11 compartments. Therefore, to determine whether CFTR resides within the Rab11a- and Rab11b-labeled vesicular compartments and thereby support our morphological observations, we immunoisolated the Rab11 vesicles biochemically and tested for the presence of endogenous CFTR. T84 cells were homogenized, and the homogenate was fractionated on a step-flotation sucrose gradient by ultracentrifugation. The 25/35% sucrose interface, which is enriched in Rab11-positive vesicles (Trischler *et al.*, 1999), was isolated and incubated with Rab11 isoform-specific antibodies. Antibody-bound endosomes were then immunoisolated with magnetic beads precoated with a secondary IgG and washed extensively. Bound vesicles were solubilized in Laemmli buffer, separated on SDS-PAGE, and immunoblotted for proteins of interest. Both Rab11a and Rab11b immunoisolations revealed an enrichment of endogenous CFTR within these vesicular compartments compared with Rab21 or a nonspecific IgG isolation (Figure 4A, top row). Immunoisolated samples were blotted for an ER-resident (Bip/GRP78) or a soluble (actin) protein to confirm the purity and specificity of the immunoisolations (Figure 4A, rows 2 and 3). Further Western blotting with a pan-Rab11 antibody that recognizes both Rab11a and Rab11b demonstrates that Rab11 endosomes were isolated successfully (Figure 4A, row 4).

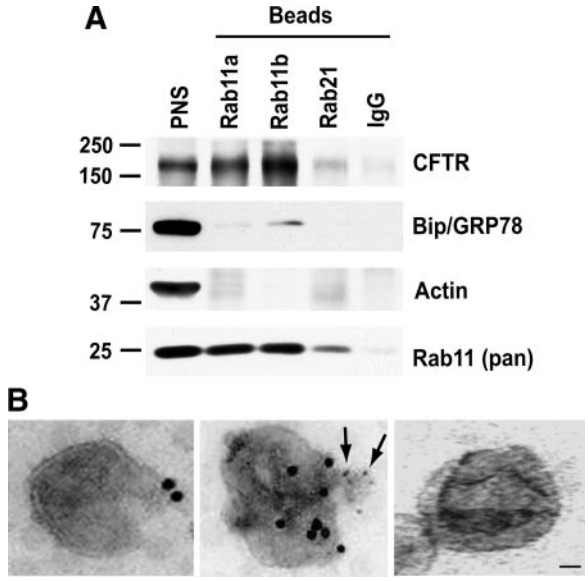

Figure 4. CFTR is present within Rab11 immunoisolated vesicles. (A) A T84 cell postnuclear supernatant (PNS) was obtained after cell homogenization, loaded on a step-floatation sucrose gradient, and centrifuged for 3 h at 108,000 × *g*. The 25/35% interface containing recycling and early endosomes was incubated with antibodies specific for Rab11a, Rab11b, Rab21, or a nonspecific IgG. Rab-positive vesicles were isolated using magnetic Dynabeads preconjugated to an anti-rabbit secondary antibody. Beads were washed, and bound vesicles were solubilized in sample buffer, separated on SDS-PAGE, and blotted for CFTR, Bip/GRP78 (ER), actin, and Rab11 (pan antibody recognizes both isoforms). A representative blot of three independent experiments is shown. (B) Rat jejunum enterocytes were isolated and homogenized as described in *Materials and Methods.* The PNS was loaded on a step-floatation sucrose gradient, and the 25/35% interface was isolated. Membranes were deposited on an EM grid, and micrographs obtained after immunogold labeling for CFTR (15 nm) or CFTR and Rab11 (5 nm, arrows). Endosomes incubated in the absence of the primary antibodies provide a negative control for the secondary immunogold labeling (right panel). Scale bar, 60 nm.

Given the colocalization of CFTR with Rab11 in rat intestine (Figure 3), we investigated whether CFTR and Rab11

could be visualized within the same endosomes. Immuno-EM examination of vesicles isolated on sucrose gradients from rat jejunum enterocytes demonstrates the presence of CFTR-positive vesicles as shown in Figure 4B (left, 15-nm gold particles). Isolated vesicles costained for CFTR and Rab11 (5-nm gold) revealed that both proteins could be localized to the same vesicle (Figure 4B, right). Thus, CFTR is present within Rab11-positive vesicles isolated from an endogenous-expression system and native tissue. These findings confirm our immunofluorescence observations.

Rab11b S25N Selectively Impairs CFTR Function in SPQ Halide Efflux Assays

To determine whether Rab11 was able to modulate CFTR function at the apical membrane, we performed SPQ halide efflux assays on T84 cells expressing Rab11 mutants. The iodide-sensitive, membrane-impermeant fluorescent indicator SPQ, which is quenched in the presence of iodide, was introduced into coverslip-grown T84 cells by hypotonic shock in the presence of a NaI buffer (Chao *et al.*, 1989). After recovery, SPQ-loaded cells were mounted on a heated microscope stage in the continued presence of NaI buffer, and changes in CFTR-mediated SPQ fluorescence were monitored during perfusion at 37°C with $NaNO_3$ buffer (which does not quench SPQ fluorescence) containing the cAMP/PKA agonist, forskolin, or with vehicle as control. As shown in Figure 5A, perfusion of cells with nitrate buffer lacking forskolin results in a minor increase in fluorescence (blue triangles), due to iodide leakage from the cells under nonstimulated conditions. However, when T84 cells were perfused with nitrate buffer containing 10 μM forskolin, cAMP/PKA-activation of CFTR yielded a robust increase in SPQ fluorescence, which results from the dequenching of SPQ as iodide exits the cells through CFTR in exchange for nitrate (red circles). The SPQ fluorescence was quenched rapidly upon reperfusion with iodide buffer, indicating reentry of iodide through still-open CFTR channels.

To verify that the cAMP-evoked increase in SPQ fluorescence resulted from iodide efflux through CFTR channels, we performed SPQ experiments in the presence of the CFTR-specific inhibitors, GlyH101 and $CFTR_{inh}172$. Although vehicle-treated cells responded robustly to agonist, similar to the data of Figure 5A, addition of the CFTR inhibitors reduced 90% of the SPQ fluorescence increase (see Supplemental Figure S1, A and B). These data confirm that SPQ fluorescence assays are a valuable technique for measuring cAMP/PKA-regulated CFTR function in T84 cells.

To test for the role of the Rab11 isoforms in regulating CFTR function, T84 cells were electroporated with GFP-fused Rab11a and/or Rab11b dominant negative (S25N) constructs. Electroporation of T84 cells provides a technique for introducing constructs into these otherwise difficult-to-transfect epithelial cells with ~75% efficiency as estimated from the GFP fluorescence at 24 h after electroporation (our unpublished observations; see *Materials and Methods*). Figure 5B shows epifluorescent images of T84 cells at the appropriate wavelength for GFP and SPQ detection for the same field of cells. ROIs were chosen for GFP-expressing cells (green circles) or for nontransfected cells, which did not express GFP (red circles). This approach allowed changes in SPQ fluorescence to be monitored in expressing and nonexpressing populations within the same field of cells. After the SPQ determinations, T84 cells were fixed and stained for ZO-1 to examine whether cells grown on glass coverslips displayed a polarized phenotype. Figure 5B (ZO-1) shows that T84 cells grown for 3–5 d on glass were able to form tight junctions similar to cells grown on transwell filters (Figure 1C).

The S25N point mutation in Rab11a and Rab11b has been shown to increase its affinity for GDP, thereby locking the Rab GTPase in an inactive, non-membrane–associated state (Ullrich *et al.*, 1996; Schlierf *et al.*, 2000). Figure 5A shows a representative SPQ tracing of GFP-Rab11b-S25N–expressing cells (green diamonds), whereas Figure 5B (SPQ) shows the corresponding SPQ image for the same field of cells at the peak of the response (6 min after forskolin addition). Note that GFP-Rab11b-S25N–expressing cells (green ROIs) show a lower SPQ fluorescence peak signal compared with the neighboring non-GFP-Rab11b-S25N–expressing cells (red ROIs), providing visualization of the signals depicted in Figure 5A. The summary figure (5C), provides the mean slope of the fluorescence increase (see Figure 5A, dashed lines) observed for cells under the three conditions examined: black bar, no agonist added; open bars, nontransfected (no GFP expression detected); and gray bars, cells expressing GFP. As shown in the first pair of bars, cAMP activation of CFTR-mediated halide efflux in GFP-transfected cells did not differ when GFP-expressing and -nonexpressing cells were compared. The same was true in GFP-Rab11a-S25N–transfected cell populations. However, cells expressing the GFP-Rab11b-S25N showed an ~80% inhibition of cAMP-stimulated CFTR activity compared with the nonexpressing cells within the same field. Coexpression of dominant negative Rab11a and Rab11b did not cause any further significant decrease in cAMP-stimulated CFTR activity over that observed for dominant negative Rab11b alone.

Because of the strong inhibition in CFTR function observed with overexpression of GFP-Rab11b-S25N, we lysed cells after SPQ assays and immunoblotted to test for possible changes in CFTR protein expression. As shown in Figure 5D and quantitated in Figure 5E, CFTR levels remained unchanged in T84 cells overexpressing the Rab11b dominant negative compared with GFP or Rab11a dominant negative cells. The expression of both of the GFP-fused Rab11 constructs (~50 kDa), and the combined signal from each endogenous Rab11 isoform (~25 kDa) are revealed by the pan-Rab11 antibody (Figure 5D, bottom panel). These findings show that the Rab11b dominant negative overexpression does not modulate total cellular levels of CFTR significantly, which suggests that its inhibition of CFTR function may reflect the regulation of membrane CFTR channel density by Rab11b. Overall, these results demonstrate that Rab11b regulates CFTR function in the plasma membrane of T84 cells and that functional Rab11b is required for CFTR-mediated halide efflux.

Rab11b Q70L Increases CFTR-mediated Anion Efflux

Studies examining the functional role of Rab GTPases in regulating membrane trafficking often also rely on the use of dominant active, GTP-locked mutants to further elucidate Rab-trafficking mechanisms. We speculated that overexpression of the Rab11b dominant active mutant, Q70L, would produce increased CFTR activity in SPQ fluorescence assays, an effect opposite to that of the dominant negative mutant. As shown in Figure 6A (bottom panel), GFP-Rab11b-Q70L–expressing T84 cells showed an increase in the rate of SPQ dequenching (iodide efflux) in response to agonist, which was evident from the steeper slope of GFP-expressing cells (black diamonds) compared with non-GFP cells (gray circles) within the same field. This difference was not observed for GFP-Rab11a-Q70L–expressing cells relative to non-GFP cells (Figure 6A, top). The absence of an increase in the plateau of SPQ fluorescence with the Rab11b mutant is most

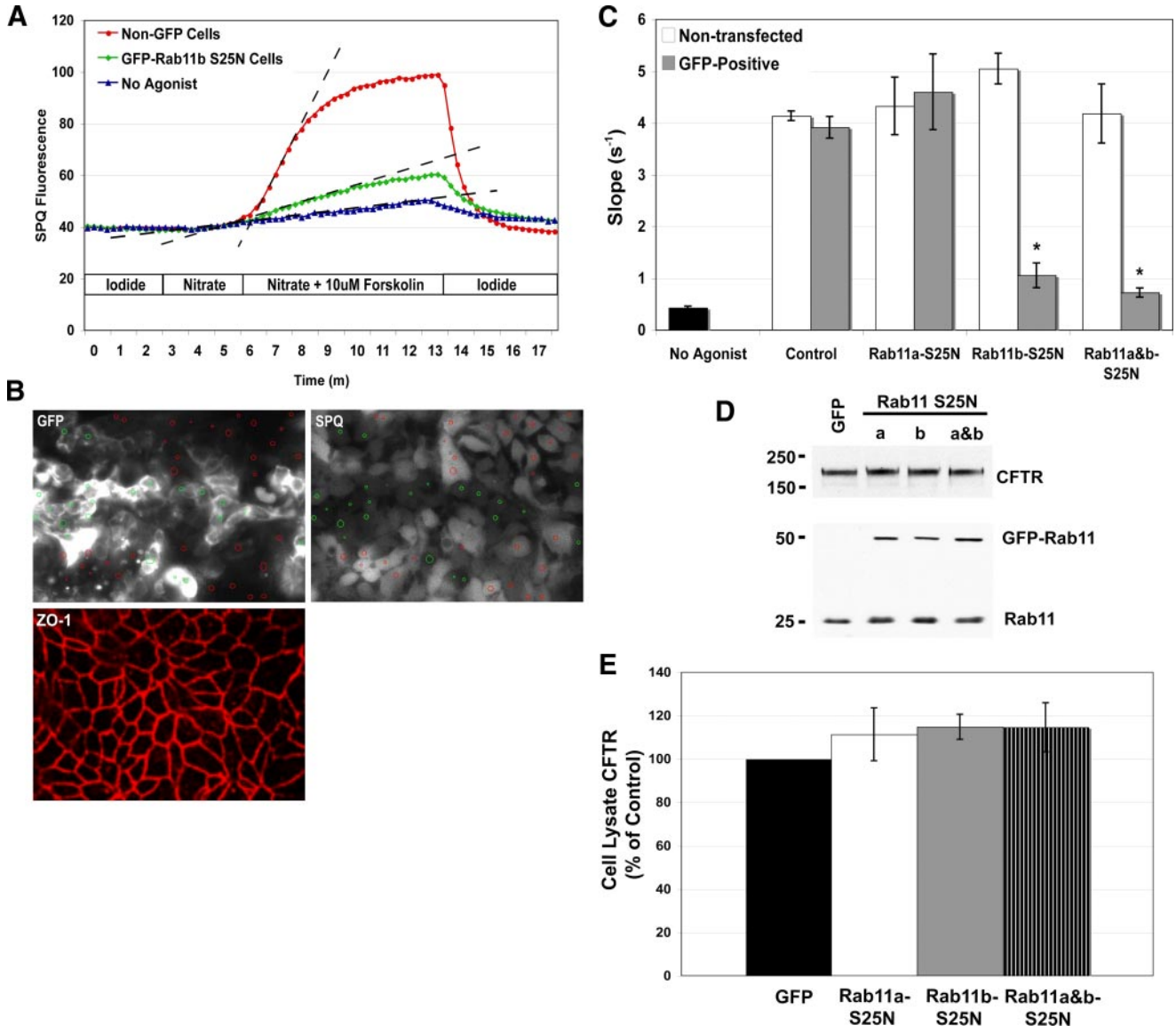

Figure 5. Dominant negative Rab11b impairs CFTR-mediated increases in halide permeability. (A) Representative SPQ fluorescence traces showing increases in normalized fluorescence units for T84 cells perfused with nitrate buffer alone (blue triangles) or nitrate buffer with 10 μM forskolin for T84 cells with (green diamonds) or without (red circles) GFP-Rab11b-S25N expression. (B) Epifluorescent images of T84 cells expressing GFP-Rab11b-S25N collected at the 520-nm (GFP) and the 445-nm (SPQ) emission wavelengths for the same field of cells. The SPQ image depicts the image obtained at the peak fluorescence observed after perfusion for 6 min with nitrate buffer containing forskolin and shows that cells expressing the GFP-Rab11b-DN construct remain dim relative to those not expressing the GFP construct. Populations of cells expressing GFP-tagged Rabs were identified with green ROI circles, whereas non-GFP cells were identified with red ROIs. Also shown is a field of T84 cells that were fixed and stained for ZO-1 after performing an SPQ experiment (ZO-1). Confocal sections reveal that ZO-1 localized to the tight junctions at the apical pole of T84 cells in the pattern characteristic of polarized cells. (C) Bars provide mean values for the maximal rate of fluorescence increase (see A, dashed lines, and *Materials and Methods*) for ROI populations from four different monolayers on coverslips (>200 cells total). Slopes were calculated for non-GFP–expressing (□) or GFP-expressing (▨) T84 cells within the same field. Data are mean ± SEM. Statistically significant differences in GFP slopes compared with non-GFP slopes; *$p < 0.01$. (D) T84 coverslips were scraped and lysed in lysis buffer immediately after SPQ experiments. Protein levels were quantitated, equal amounts of protein were loaded and separated by SDS-PAGE, and proteins were then transferred to PVDF for Western blotting. The 50-kDa band, as detected by the pan Rab11 antibody, represents the expression levels of the GFP-tagged Rab11 isoforms compared with the combined (a&b) endogenous levels (25 kDa). (E) Quantitation of Western blots reveals that CFTR protein levels are not altered significantly with overexpression of GFP-Rab11a- and/or b-S25N compared with GFP ($n = 3$, $p > 0.05$).

likely due to saturation of dye fluorescence intensity, which is reached more rapidly in cells expressing the active form of Rab11b. To display the summary data, we calculated the rate constants by fitting the increases in SPQ fluorescence observed between the 6.5- and 11-min time intervals to a single-exponential function. Figure 6B shows the mean rate constants for GFP-Rab11a- or b-Q70L–expressing cells (GFP-positive) compared with nonexpressing cells (Non-transfected) for more than 200 cells from four different monolayers for each group. These data show that overexpression of the dominant active Rab11b increases the kinetics of the CFTR-mediated SPQ fluorescence response.

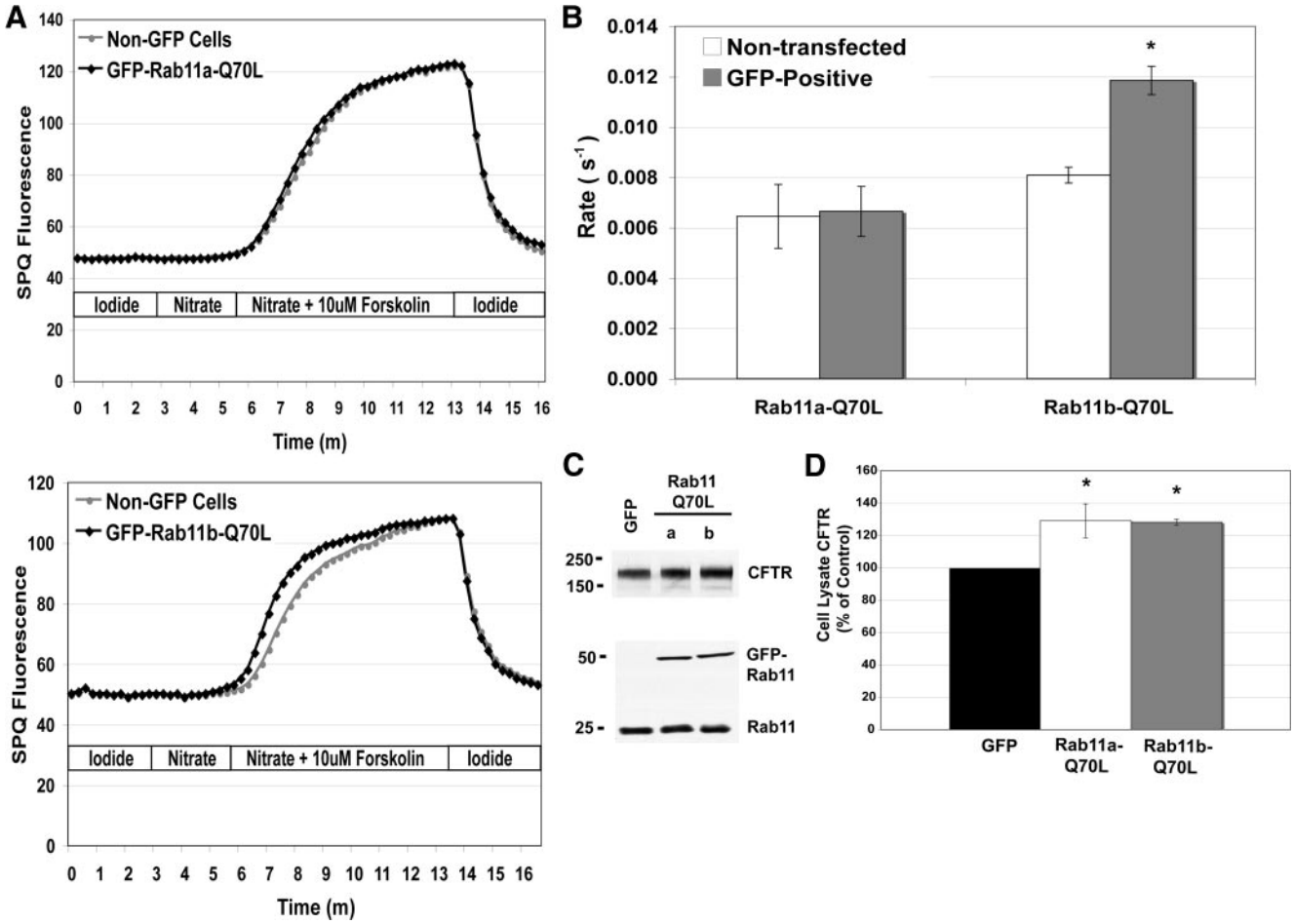

Figure 6. Dominant active Rab11b accelerates the CFTR-mediated halide permeability response to agonist. (A) Representative SPQ fluorescence traces (mean of 40 cells) for GFP-Rab11a- (top panel) or Rab11b-Q70L- (bottom panel) expressing cells (black diamonds) compared with non-GFP–expressing cells (gray circles) within the same field, show an increased response rate for the GFP-Rab11b-Q70L–expressing cells. (B) Rate constants were calculated from the mean rates from four different monolayers (>200 cells) using a single-exponential function (see *Materials and Methods*) for the two populations. Data are mean ± SEM. Significantly different from non-GFP–expressing cells; *$p < 0.01$. (C and D) Western blot analysis of lysates obtained from T84 cells used for SPQ experiments shows that total CFTR levels in GFP-Rab11a-Q70L– and GFP-Rab11b-Q70L–expressing cells increase by 29 ± 10 and 28 ± 2%, respectively. Significantly different value relative to non-GFP–expressing cells; *$p < 0.005$.

To examine CFTR protein levels within dominant active-expressing cells, Western blotting for CFTR was performed on lysates obtained from cells used for SPQ experiments. Unlike the dominant negative mutant, we detected a minor but significant increase in the steady-state CFTR protein levels in both of the dominant active Rab11a and Rab11b cell populations compared with GFP-transfected cells (Figure 6, C and D). These results suggest that overexpression of the dominant active Rab11 isoforms influences endogenous CFTR expression levels; however, only overexpression of the Rab11b dominant active yielded an increase in the rate of SPQ dequenching in the halide efflux experiments.

Dominant Negative Rab11b Expression Inhibits CFTR Chloride Secretion across Polarized T84 Monolayers

T84 cells seeded onto semipermeable transwell supports form polarized monolayers that develop high levels of TER, enabling them to generate vectorial chloride secretion similar to the native intestinal epithelium (Dharmsathaphorn *et al.*, 1984). The asymmetric distribution of ion transporters and channels that mediate net transepithelial movement of ions have been described thoroughly in this system, and it is well accepted that CFTR provides the primary exit pathway for chloride secretion across the apical membrane in polarized T84 cell monolayers (reviewed in Barrett, 1993). Therefore, this system serves as an ideal model for testing the contribution of apical CFTR traffic regulation to the secretory function of the epithelium. To examine whether Rab11b regulates CFTR function in a fully polarized cell system, Isc measurements were performed in Ussing chambers using T84 epithelia transduced with adenoviruses that express GFP, GFP-Rab11a-S25N, or GFP-Rab11b-S25N. Figure 7A shows representative Isc tracings for GFP- (black), GFP-Rab11a-S25N– (light gray), or GFP-Rab11b-S25N (dark gray)–expressing cells and reveals a robust inhibition of forskolin-activated, CFTR-conducted chloride current in the dominant negative Rab11b-transduced monolayer as compared with the GFP- or GFP-Rab11a-S25N–transduced monolayer. Addition of bumetanide to block the basolateral Na^+-K^+-$2Cl^-$ (NKCC1) cotransporter inhibited the Isc by blocking chloride uptake across the basolateral membrane, which is required for chloride secretion. The summary fig-

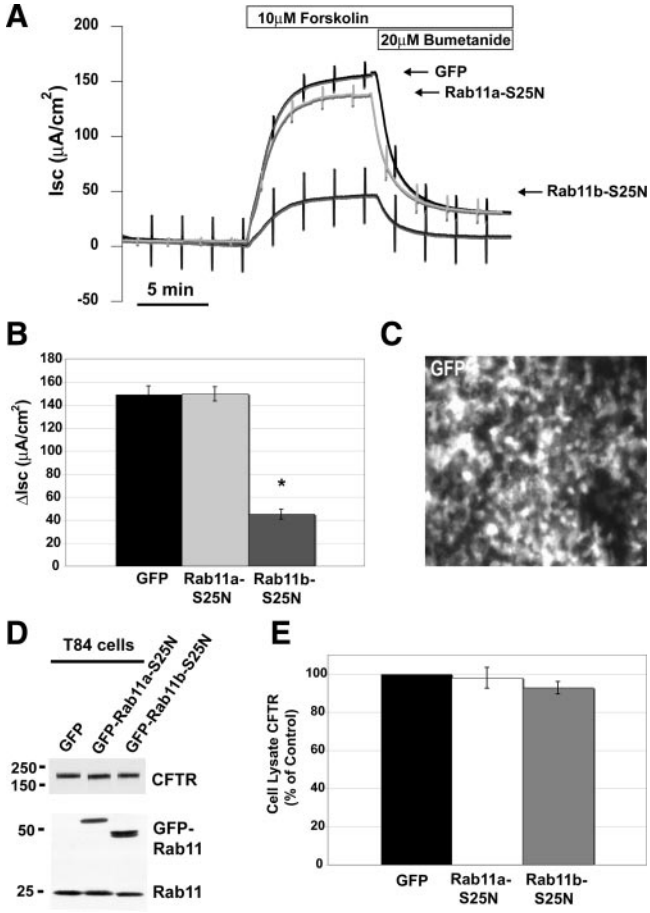

Figure 7. Dominant negative Rab11b expression inhibits Isc in polarized T84 cell monolayers. (A) Representative Isc traces recorded from T84 monolayers transduced with GFP (black), GFP-Rab11b-S25N (light gray), or GFP-Rab11a-S25N (dark gray) show that only dominant negative Rab11b strongly inhibits forskolin-activated CFTR chloride currents. (B) Bars provide mean (± SEM) changes in CFTR-mediated Isc for GFP- (black), GFP-Rab11a-S25N– (light gray), or GFP-Rab11b-S25N– (dark gray) expressing T84 cell monolayers ($n = 6$). *$p < 0.0003$. (C) Image depicts fluorescent capture of T84 cell monolayer before current measurements demonstrating robust expression of GFP-Rab11b-S25N. Similar micrographs were evidenced for GFP and GFP-Rab11a-S25N cells (not shown). (D) Western blot of T84 lysates obtained after Isc measurements on GFP, GFP-Rab11a-S25N and GFP-Rab11b-S25N. GFP-tagged Rab11 mutants detected at the expected 50-kDa molecular weight with a pan-Rab11 antibody reveals similar expression of each dominant negative Rab11 isoform. (E) Quantitation of whole cell lysate protein levels reveal that total cellular CFTR levels (±SEM) in GFP-Rab11a-S25N and GFP-Rab11b-S25N cells remain unchanged relative to GFP control ($n = 4$, $p > 0.1$).

ure (7B) shows the mean change in forskolin-induced Isc across adenovirus-transduced T84 monolayers expressing GFP (black bar), GFP-Rab11a-S25N (light gray bar), or GFP-Rab11b-S25N (dark gray bar).

In agreement with our SPQ data (Figure 5C), the dominant negative Rab11a construct failed to inhibit the forskolin-stimulated increase in Isc compared with GFP-expressing control monolayers. However, overexpression of the dominant negative Rab11b reduced CFTR-mediated chloride secretion by ~70%, compared with the control GFP expressing monolayers. The ability of the GFP-Rab11a-S25N virus to inhibit apical recycling through the ARE was verified because it was shown to block dimeric IgA recycling in polarized MDCK cells (Dr. A. Oztan, personal communication; data not shown). Visual inspection of the transduced cell monolayers by epifluorescence microscopy before Ussing chamber experiments allowed an approximation of expression for the virally delivered constructs. An epifluorescent image of a T84 monolayer expressing GFP-Rab11b-S25N is shown in Figure 7C, which demonstrates the high percentage of cells transduced. To examine whether the robust inhibition in CFTR-mediated current was a result of decreased total cell CFTR expression, we lysed cells from transwell supports after Ussing chamber experiments and performed Western blots for CFTR and Rab11. As shown in Figure 7D and quantitated in 7E, endogenous CFTR protein levels in T84 monolayers remained unaltered with adenovirus-mediated overexpression of either dominant negative Rab11 isoform compared with GFP expressing T84 cells. The pan Rab11 antibody was used to detect both GFP-fused Rab11 isoforms in addition to the endogenous Rab11 isoforms. These results demonstrate the selective requirement for the Rab11b isoform function in supporting regulated, CFTR-mediated transepithelial chloride secretion across polarized T84 cell monolayers.

Dominant Negative Rab11b Expression Decreases CFTR Protein Expression at the Apical Membranes of Polarized T84 Monolayers

To determine whether the reduction in transepithelial chloride transport across T84 epithelia reflects Rab11b modulation of CFTR density at the apical membrane, we used cell surface biotinylation to examine the levels of endogenous CFTR present at the apical surface of polarized T84 monolayers transduced to express GFP, GFP-Rab11a-S25N, or GFP-Rab11b-S25N. Epifluorescent inspection of GFP expression in monolayers 24 h after adenoviral transduction revealed similar expression efficiency as evidenced in monolayers used for the Isc measurements (Figure 7C; data not shown). In addition, measurements taken 24 h after transduction showed recovery of the TER of T84 monolayers to ~75% of that recorded before tight junction disruption and viral transduction (data not shown; see *Materials and Methods*). As shown in Figure 8A, biotinylation of the apical membrane followed by streptavidin-mediated precipitation and CFTR immunoblotting revealed a significant decrease in apical membrane CFTR protein levels in GFP-Rab11b-S25N cells compared with GFP- or GFP-Rab11a-S25N–expressing T84 cells (top panel). Quantitation showed a 49 ± 13% decrease in the apical membrane CFTR compared with GFP or GFP-Rab11a-S25N cells (Figure 8B). Western blot analysis of the input used for biotin pulldown showed that total CFTR levels were unaltered (Figure 8A, second row), which is in agreement with the total cellular CFTR levels measured in cells used for Isc measurements (Figure 7, D and E). These results show that Rab11b, not Rab11a, regulates CFTR channel density at the apical membranes of polarized T84 intestinal epithelial cells under cAMP/PKA stimulation conditions. The magnitude of this reduction in apical CFTR suggests that it is responsible primarily for the inhibition of the Isc elicited by the expression of the dominant negative Rab11b.

Dominant Negative Rab11b Inhibits Apical Recycling of CFTR in Polarized Intestinal Epithelial Cells

Given the efficient apical recycling of endogenous CFTR in polarized epithelial cells and the well-described role for Rab11a in membrane recycling, we speculated that Rab11b may also function as a regulator of apical membrane recy-

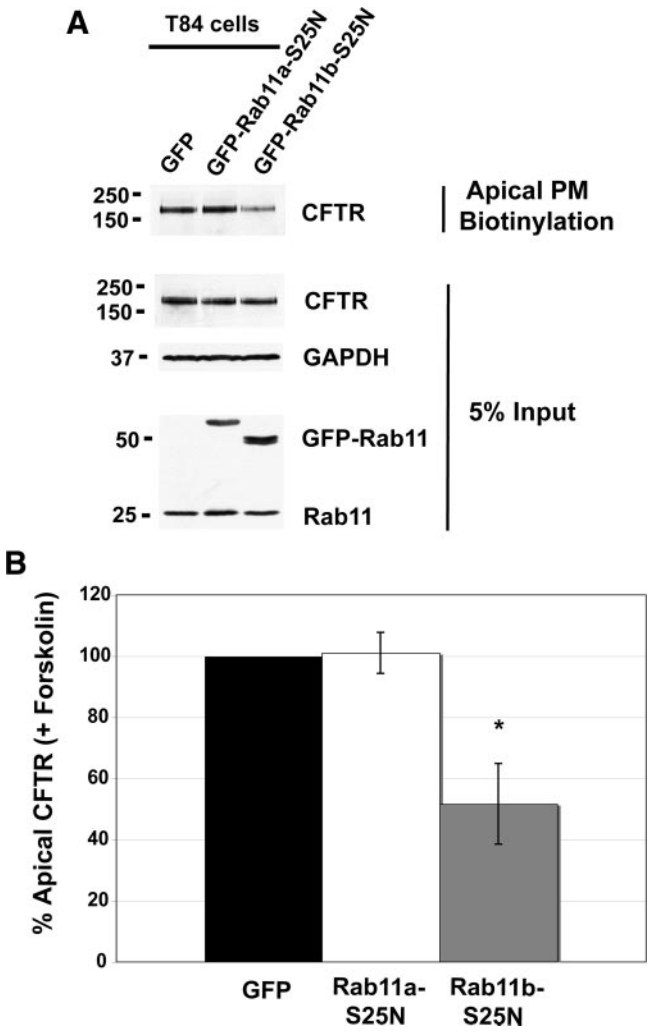

Figure 8. Dominant negative Rab11b overexpression decreases apical membrane CFTR in polarized T84 cells. (A) Representative CFTR Western blot following apical membrane biotinylation and streptavidin pull down shows decreased cell surface CFTR in GFP-Rab11b-S25N expressing cells relative to the GFP control or GFP-Rab11a-S25N expressing monolayers. To mirror the apical CFTR density measurements with the functional analysis reported in Figure 7, biotinylation was performed after a 10 min stimulation of the epithelia with 10 μM forskolin. Western blotting of 5% of the precipitate (input) reveals that total CFTR levels remain unchanged (see Figure 7E); GAPDH was used as loading control. Immunoblotting with pan-Rab11 antibody demonstrates the expression of endogenous Rab11 and both dominant negative GFP-fused Rab11 isoforms. (B) Quantitation of apical membrane CFTR from biotinylation of polarized T84 cells transduced with GFP, GFP-Rab11a-S25N or GFP-Rab11b-S25N (n = 3), showing that the Rab11b dominant negative construct decreases the mean levels of apical membrane CFTR by 48 ± 13%, relative to the GFP control. *$p < 0.05$.

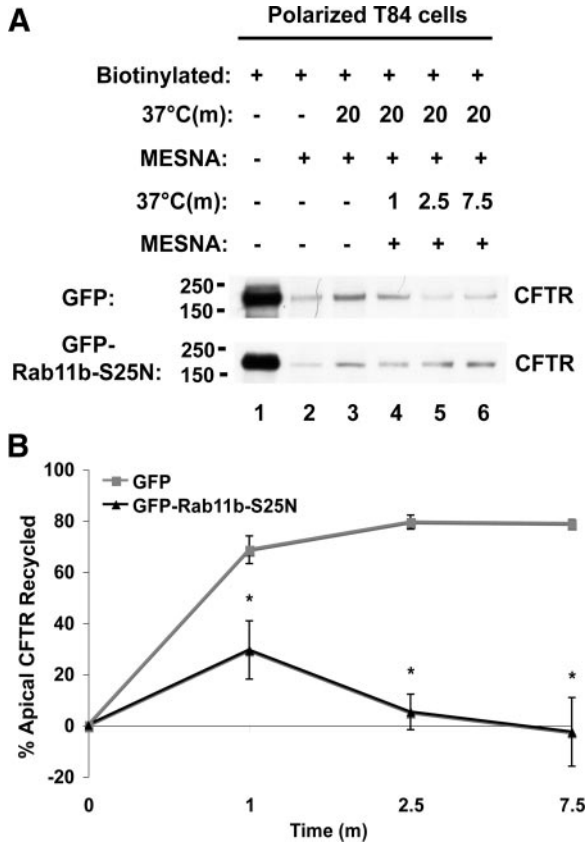

Figure 9. Dominant negative Rab11b inhibits the apical recycling of endogenous CFTR in polarized T84 cells. (A) Representative CFTR blots obtained from biotin protection assays utilized to measure CFTR recycling in polarized T84 cells transduced with GFP (top row, exposure time = 30 s) or GFP-Rab11b-S25N (bottom row, exposure time = 45 s; see *Materials and Methods*). Lane 1, the total apical membrane CFTR that was biotinylated at 4°C; lane 2, the MESNA stripping buffer removes biotin from the apical monolayer surface efficiently (at 4°C) by reduction of the disulfide bond in the cleavable biotin reagent. Lane 3, the amount of cell surface-biotinylated CFTR internalized during 20 min at 37°C; lanes 4, 5, and 6, the internalized CFTR that remains in the cells at 1, 2.5, and 7.5 min, respectively; that is, the difference between lanes 3 and 4, 5, or 6 represents recycled CFTR. Note that the biotinylated CFTR in GFP-expressing cells is protected from the MESNA reducing agent after internalization (lane 3), but becomes sensitive again after recycling to the cell surface as indicated by the progressive decrease in band intensity seen in lanes 4, 5, and 6 (top row). T84 monolayers overexpressing dominant negative Rab11b accumulate MESNA-resistant biotinylated CFTR, indicating its failure to recycle (bottom row, lanes 4, 5, and 6). (B) Quantitation of apical CFTR recycling for GFP (▨) and GFP-Rab11b-S25N (▲) expressing T84 monolayers (GFP-Rab11b-S25N, n = 3; GFP, n = 5). *Significantly different value for GFP-Rab11b-S25N recycling as compared with CFTR recycling in GFP control monolayers (1 min = $p < 0.05$, 2.5 min = $p < 0.001$, 7.5 min = $p < 0.005$). CFTR recycling values obtained at 1, 2.5, or 7.5 min for GFP-Rab11b-S25N–expressing monolayers are not significantly different from one another; $p > 0.1$.

cling. Therefore, the apical recycling of endogenous CFTR in polarized T84 monolayers transduced to express either GFP or GFP-Rab11b-S25N was examined using a biotin protection assay as described in *Materials and Methods*. As shown in Figure 9A (see figure legend) and quantitated in Figure 9B, endogenous CFTR recycled rapidly in GFP-transduced control cells (gray squares), with ~68% of the biotin-labeled, internalized CFTR returning to the apical surface after 1 min in the presence of forskolin. However, only 5% of apical CFTR recycled at 2.5 min in GFP-Rab11b-S25N–expressing cells (black triangles), compared with ~80% recycling in control, GFP-expressing cells. Together, the results from dominant negative construct expression show that CFTR requires the selective function of Rab11b to maintain proper CFTR channel density at the apical membrane and that this is accomplished by its efficient and rapid recycling through a Rab11b-regulated pathway.

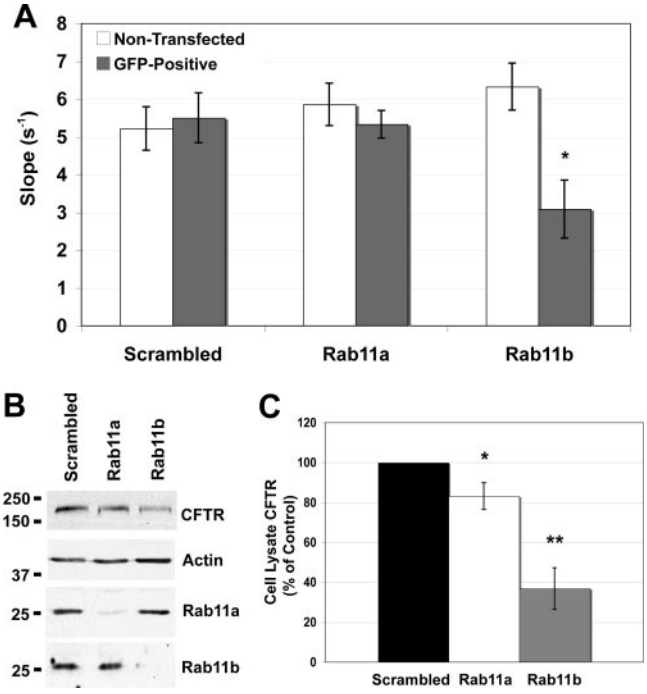

Figure 10. shRNA knockdown of Rab11b inhibits CFTR-mediated halide efflux from T84 cells. (A) Mean values for the maximal slope of the SPQ fluorescence increase (halide efflux) for ROI populations of T84 monolayers, as follows: nontransfected, non-GFP–expressing (□) or GFP-expressing (▨) cells imaged within the same field (see *Materials and Methods* and Figure 5 legend). Mean data were derived from three monolayers each; >100 cells total; mean ± SEM. Statistically significant difference in SPQ response, *p = 0.01. (B) T84 coverslips were scraped and solubilized in lysis buffer immediately after SPQ experiments. Protein levels were quantitated and equal amounts of protein were loaded and separated by SDS-PAGE. Knockdown of the individual Rab11 isoforms was confirmed using isoform-specific Rab11a or Rab11b antibodies, as shown. (C) Quantitation of the total cellular CFTR in Rab11 isoform knockdown cells. Knockdown of either Rab11a or Rab11b decreases the endogenous CFTR protein expression by 17 ± 7 or 63 ± 10%, respectively; *$p < 0.05$, **$p < 0.005$; $n = 4$.

shRNA-mediated Knockdown of Rab11b Inhibits CFTR-mediated Increases in SPQ Fluorescence in T84 Cells

Work done to examine the effector protein binding properties for each of the Rab11 isoforms suggested that they may share common downstream effectors because of their high level of similarity (Junutula *et al.*, 2004). To confirm that our results obtained with the dominant negative Rab11b overexpression were not a result of impairing indirectly the function of Rab11a and to determine whether Rab11b protein expression is required for recycling of endogenous CFTR, we performed SPQ fluorescence assays on T84 cells depleted of either Rab11 isoform using shRNA-mediated knockdown. Figure 10A shows the results of SPQ fluorescence experiments performed on T84 cells expressing GFP-tagged shRNA constructs for a scrambled, nonspecific sequence or specific for Rab11a or Rab11b. Data from nontransfected, control cells (open bars) within the same field as the GFP-positive, shRNA knockdown cells (gray bars) is provided as the slope of the increase in SPQ fluorescence dequenching. Neither scrambled nor Rab11a shRNA-expressing knockdown cell populations (GFP-positive) differed significantly from nontransfected cells when the slopes of the SPQ fluorescence increase in response to forskolin were compared. However, cells with reduced Rab11b expression showed a 53 ± 14% reduction in agonist-evoked halide efflux, again demonstrating isoform specificity in the Rab11 effect on CFTR function. Western blotting with Rab11a- or Rab11b-specific antibodies of T84 lysates collected after SPQ experiments confirmed significant knockdown of Rab11a or Rab11b (Figure 10B). In addition, steady-state levels of CFTR were reduced differentially by knockdown of Rab11a or Rab11b: 17 ± 7 or 63 ± 10%, respectively. These isoform-specific knockdown results support our previous conclusions, drawn from the mutant Rab11b experiments, and suggest that expression of Rab11b, but not Rab11a, is required to control the CFTR density at the membranes of T84 cells.

DISCUSSION

CFTR is a dynamic protein within the apical membrane of epithelial cells, where it undergoes rapid and efficient endocytic internalization and recycling back to the cell surface (Bertrand and Frizzell, 2003; Ameen *et al.*, 2007). Extensive data from our own work and numerous other investigators has demonstrated the importance of CFTR recycling in the maintenance of apical membrane CFTR (reviewed in Bertrand and Frizzell, 2003). CFTR internalization and recycling rates influence both plasma membrane copy number and the channel's functional half-life directly, and therefore, these processes directly impact CFTR-mediated anion secretion. Herein, we tested the hypothesis that a member of the Rab family of small GTPases functions to maintain appropriate CFTR density at the apical membrane in polarized epithelial cells by facilitating its efficient recycling.

We demonstrate that Rab11b, a member of the Rab11 family of GTPases, regulates the intracellular recycling of CFTR in polarized T84 epithelial cells. Our immunofluorescent staining for CFTR revealed punctate structures localized at and beneath the TJ marker, ZO-1, suggesting endogenous CFTR localization at the plasma membrane and within subcellular compartments. These findings agree with the biochemical data obtained from studies performed previously in T84 cells (Prince *et al.*, 1994). In addition, we show that a portion of this CFTR colocalized with both Rab11a- and Rab11b-labeled vesicles at the apical pole of T84 epithelial cells. The localization of CFTR to Rab11 positive compartments was confirmed by the immunoisolation of both Rab11a- and Rab11b-containing vesicles from T84 cells and immuno-EM on Rab11 vesicles isolated from rat jejunal enterocytes, which demonstrates the presence of endogenous CFTR within these subcellular compartments, not only in cell culture but also in vivo.

Despite the observation that CFTR colocalized with both Rab11a and Rab11b, our results from halide efflux measurements and transepithelial chloride secretion across polarized T84 monolayers show that only Rab11b is involved in maintaining functional CFTR at the apical plasma membrane. Diminished CFTR function produced by overexpression of the dominant negative Rab11b could not be explained by alterations in CFTR biosynthesis or degradation, as whole cell CFTR protein levels remained unchanged. However, the strong inhibition of CFTR function observed suggested that it was depleted from the apical membrane; therefore, we used biochemical assays to examine endogenous CFTR channel localization and recycling. Our biotinylation experiments revealed that CFTR channel density within the apical plasma membrane is modulated through a Rab11b-dependent recycling pathway. Additionally, in knockdown exper-

iments, only cells depleted of Rab11b, not Rab11a, exhibited a reduced CFTR-mediated SPQ fluorescence response upon agonist addition, demonstrating the physiological significance of Rab11b expression for apical CFTR function. These knockdown results suggest that the effects of the dominant negative Rab11b overexpression on CFTR recycling are not due to perturbations of other pathways, such as an indirect effect on Rab11a function.

Interestingly, knockdown of Rab11b also resulted in a significant decrease in CFTR protein expression. A similar affect was reported for the C-type lectin, Langerin, in HeLa and M10–22E cells, as either overexpression of the dominant negative Rab11a, or its depletion, resulted in decreased Langerin protein expression (Uzan-Gafsou *et al.,* 2007). Further investigation revealed that Rab11a expression and function were required for the formation of Birbeck Granules, a specialized subdomain of the recycling compartment that facilitates Langerin recycling in Langerhans cells. In the absence of Rab11a expression or function, Langerin was targeted for lysosomal degradation. Likewise, Rab11b expression may be required for the establishment or stability of a recycling compartment within T84 cells that recruits CFTR molecules that are destined for apical recycling, similar to that reported for Langerin. If so, it will be interesting to determine whether the lack of Rab11b expression targets endocytosed CFTR to the degradative, rather than the recycling, pathway.

However, unlike the Langerin studies, overexpression of the GDP-locked Rab11b mutant in T84 cells did not affect endogenous CFTR expression levels significantly. This may be due to the retention of recycling capability by natively expressed Rab11b, providing a pathway to which CFTR may be recruited but not recycled. This outcome could prevent its appropriate localization and function at the apical membrane without resulting in altered whole cell expression levels. Conversely, CFTR may be shuttled to the unperturbed Rab11a compartment, rather than to a degradative pathway. Further work is required to elucidate the disparities observed between the knockdown and dominant negative effects on CFTR protein expression reported herein.

Rab11 Isoform Comparisons

Rab11b has not received the attention given its near relative, Rab11a, particularly in regard to protein recycling. Early studies had implicated a role for Rab11b, similar to that ascribed to Rab11a, because it regulated transferrin receptor recycling in nonpolarized 293 cells (Schlierf *et al.,* 2000). In polarized cell models (e.g., MDCK cells), Rab11b localized to a subapical vesicular compartment, distinct from that for Rab11a or the known apical recycling cargoes, H^+-K^+-ATPase and pIgR. These findings suggested that Rab11b was localized to a compartment that is different from the Rab11a-identified ARE (Lapierre *et al.,* 2003). Furthermore, Rab11b staining did not overlap with staining for internalized transferrin receptor, which localizes to the subapical common recycling endosomes in polarized MDCK cells, confirming also that it did not associate with this perinuclear recycling compartment (Leung *et al.,* 2000; Lapierre *et al.,* 2003). These data suggest the existence of two separate apical Rab11 recycling compartments within polarized epithelial cells. Our results establish the requirement for Rab11b expression and function in CFTR recycling in a polarized epithelial system, demonstrating that this process is independent of Rab11a. From these studies, however, we are unable to address further whether Rab11a and Rab11b form distinct recycling compartments or whether they demarcate functionally distinct subdomains of the same interconnected recycling network, as described previously for Rab4, Rab5, and Rab11 (Sonnichsen *et al.,* 2000). Identification of additional cargos that utilize these isoform-specific apical recycling pathways should further elucidate potential interplay in cargo handling between the Rab11a and Rab11b recycling compartments.

It was surprising that manipulation of the Rab11a isoform, which shares 89% amino acid sequence homology with Rab11b, failed to affect the apical membrane recycling of CFTR. The crystal structures of Rab11a and Rab11b show significant differences, including the presence of 11a as a dimer in the crystal structure, whereas 11b crystallized as a monomer. In addition, there were differences in subdomain orientations and helical region exposure that were interpreted to suggest different GTP hydrolysis rates in these isoforms (Scapin *et al.,* 2006). These factors may lead to differences in downstream effector binding that account for functional disparities, as revealed by our data. Consistent with this concept, one study examined Rab11 isoform associations with the Rab11 family of interacting proteins (FIPs) and attempted to differentiate between Rab11a and Rab11b isoforms (Junutula *et al.,* 2004). Although they suggest that the FIPs could not differentiate between Rab11a or Rab11b in their active, GTP-bound conformations, not all members of the FIP family were examined in those studies, and it is also possible that other, as-yet unidentified Rab11-interacting proteins could mediate specific Rab11a or Rab11b downstream functions.

Cell Type–dependent Recycling Pathways

It is well appreciated that trafficking pathways inherent to nonpolarized cells do not mirror the pathways of more complex polarized epithelial systems (Tuma *et al.,* 2002). Recent studies have examined CFTR trafficking itineraries in nonpolarized heterologous expression systems and have noted colocalization with and regulation by specific trafficking regulators, including Rab GTPases (Gentzsch *et al.,* 2004) and SNARE proteins (Bilan *et al.,* 2004). Although such studies provide proof-of-concept for a functional role of Rab GTPases in CFTR trafficking, they do not necessarily elucidate the trafficking components that are operative in the polarized epithelia where CFTR functions. Examples of disparities between data obtained from epithelial and nonepithelial systems include functions of protein trafficking and biogenesis mechanisms (Denning *et al.,* 1992; Bertrand and Frizzell, 2003; Varga *et al.,* 2004; Ameen *et al.,* 2007).

Indeed, it is possible that the cellular context could affect the manner in which CFTR is handled, even within different types of epithelial cells. For example, a study by Swiatecka-Urban *et al.* (2005) examined apical membrane CFTR trafficking in human bronchial epithelial cells (CFBE41o-) that were transduced with lentivirus to express WT or ΔF508 CFTR (Bebok *et al.,* 2005). The use of dominant negative or dominant active Rab11a constructs suggested that Rab11a regulated the cell surface density of CFTR in these polarized airway cells. Rab11b expression and function were not addressed in that work. Nevertheless, in relation to the present work, those studies suggested that CFTR recycling is regulated by Rab11a, and this comparison suggests that Rab isoform regulation may be cell type-specific, differing even when epithelia from different tissues are compared. Interestingly, although no significant Rab11a effect on CFTR function or localization at the apical membrane was detected in our intestinal cell studies, overexpression of the dominant active Rab11a or Rab11a knockdown both affected CFTR expression levels. These alterations in the steady-state protein levels of endogenous CFTR verify detection of CFTR within the ARE, as shown by our immunofluorescence and

immunoisolation data. Therefore, additional work will be required to determine the significance of the Rab11a-localized CFTR within this epithelial cell model. These comparative observations highlight the complexity of Rab11 recycling compartments and suggest that further studies of these systems may also reveal differences in Rab isoform effector proteins.

Some evidence (Bertrand and Frizzell, 2003; Guggino and Stanton, 2006) is consistent with the concept that cAMP/PKA agonists redistribute CFTR from intracellular compartments to the apical membranes and that this regulated trafficking of CFTR occurs in intestinal, but not airway, cells. Thus, it is possible that Rab11b mediates an agonist-sensitive, regulated recycling pathway, which is supported by this work. Our results demonstrating Rab11b dependence in intestinal epithelial cells utilized forskolin stimulation of cAMP levels to examine CFTR function, localization, and recycling. From this, it is tempting to speculate that CFTR localized to the Rab11a compartment in polarized T84 cells may be trafficked in an agonist-independent, constitutive manner. If this is true, then stimulation of the Rab11b pathway by cAMP/PKA may have masked a role for Rab11a in constitutive CFTR trafficking. The implication that these isoforms may participate in specialized recycling itineraries, possibly even varying between epithelial cell types, necessitates additional work.

Finally, additional studies have shown that the transit of CFTR out of the recycling compartment is regulated by Rab11 interactions with the class V family of myosin motors. For instance, further evidence from CFBE airway cells shows a role for Rab11a interactions with myosin Vb in CFTR recycling, including data from siRNA-mediated knockdown of myosin Vb (Swiatecka-Urban *et al.*, 2007). It will be interesting to determine whether myosin Vb, or another motor isoform, facilitates Rab11b-mediated recycling, as myosin Vb appears also to bind Rab11b (Lapierre *et al.*, 2001). Future work should focus on elucidating the functional differences between these two highly similar, yet functionally distinct, Rab11 isoforms. In summary, our results show that Rab11b, not Rab11a, regulates CFTR recycling at the apical membranes of polarized intestinal epithelial cells, revealing a novel role for Rab11b in apical recycling.

ACKNOWLEDGMENTS

We gratefully acknowledge the technical assistance of Julie Bindas in the laboratory of Jay Kolls in the production of Rab11b adenoviruses. This work was supported by National Institutes of Health Grants DK073486 (N.A.B.) and DK68196 and 72506 (R.A.F.), by Cystic Fibrosis Foundation Grant BRADBU05G0 (N.A.B.), and by fellowship support from the Cystic Fibrosis Foundation (M.R.S.).

REFERENCES

Ameen, N., and Apodaca, G. (2007). Defective CFTR apical endocytosis and enterocyte brush border in myosin VI-deficient mice. Traffic *8*, 998–1006.

Ameen, N., Silvis, M., and Bradbury, N. A. (2007). Endocytic trafficking of CFTR in health and disease. J. Cyst. Fibros. *6*, 1–14.

Ameen, N. A., Ardito, T., Kashgarian, M., and Marino, C. R. (1995). A unique subset of rat and human intestinal villus cells express the cystic fibrosis transmembrane conductance regulator. Gastroenterology *108*, 1016–1023.

Ameen, N. A., Marino, C., and Salas, P. J. (2003). cAMP-dependent exocytosis and vesicle traffic regulate CFTR and fluid transport in rat jejunum in vivo. Am. J. Physiol. Cell Physiol. *284*, C429–C438.

Ameen, N. A., Martensson, B., Bourguinon, L., Marino, C., Isenberg, J., and McLaughlin, G. E. (1999). CFTR channel insertion to the apical surface in rat duodenal villus epithelial cells is upregulated by VIP in vivo. J. Cell Sci. *112*(Pt 6), 887–894.

Ameen, N. A., van Donselaar, E., Posthuma, G., de Jonge, H., McLaughlin, G., Geuze, H. J., Marino, C., and Peters, P. J. (2000). Subcellular distribution of CFTR in rat intestine supports a physiologic role for CFTR regulation by vesicle traffic. Histochem. Cell Biol. *114*, 219–228.

Barrett, K. E. (1993). Positive and negative regulation of chloride secretion in T84 cells. Am. J. Physiol. *265*, C859–C868.

Barrett, K. E., and Keely, S. J. (2000). Chloride secretion by the intestinal epithelium: molecular basis and regulatory aspects. Annu. Rev. Physiol. *62*, 535–572.

Bebok, Z., Collawn, J. F., Wakefield, J., Parker, W., Li, Y., Varga, K., Sorscher, E. J., and Clancy, J. P. (2005). Failure of cAMP agonists to activate rescued deltaF508 CFTR in CFBE41o- airway epithelial monolayers. J. Physiol. *569*, 601–615.

Bell, C. L., and Quinton, P. M. (1992). T84 cells: anion selectivity demonstrates expression of Cl- conductance affected in cystic fibrosis. Am. J. Physiol. *262*, C555–C562.

Berger, H. A., Anderson, M. P., Gregory, R. J., Thompson, S., Howard, P. W., Maurer, R. A., Mulligan, R., Smith, A. E., and Welsh, M. J. (1991). Identification and regulation of the cystic fibrosis transmembrane conductance regulator-generated chloride channel. J. Clin. Invest. *88*, 1422–1431.

Bertrand, C. A., and Frizzell, R. A. (2003). The role of regulated CFTR trafficking in epithelial secretion. Am. J. Physiol. Cell Physiol. *285*, C1–C18.

Bilan, F., Thoreau, V., Nacfer, M., Derand, R., Norez, C., Cantereau, A., Garcia, M., Becq, F., and Kitzis, A. (2004). Syntaxin 8 impairs trafficking of cystic fibrosis transmembrane conductance regulator (CFTR) and inhibits its channel activity. J. Cell Sci. *117*, 1923–1935.

Bradbury, N. A., and Bridges, R. J. (1994). Role of membrane trafficking in plasma membrane solute transport. Am. J. Physiol. *267*, C1–C24.

Bradbury, N. A., Cohn, J. A., Venglarik, C. J., and Bridges, R. J. (1994). Biochemical and biophysical identification of cystic fibrosis transmembrane conductance regulator chloride channels as components of endocytic clathrin-coated vesicles. J. Biol. Chem. *269*, 8296–8302.

Butterworth, M. B., Edinger, R. S., Johnson, J. P., and Frizzell, R. A. (2005). Acute ENaC stimulation by cAMP in a kidney cell line is mediated by exocytic insertion from a recycling channel pool. J. Gen. Physiol. *125*, 81–101.

Casanova, J. E., Wang, X., Kumar, R., Bhartur, S. G., Navarre, J., Woodrum, J. E., Altschuler, Y., Ray, G. S., and Goldenring, J. R. (1999). Association of Rab25 and Rab11a with the apical recycling system of polarized Madin-Darby canine kidney cells. Mol. Biol. Cell *10*, 47–61.

Chan, H. C., Kaetzel, M. A., Nelson, D. J., Hazarika, P., and Dedman, J. R. (1992). Antibody against a cystic fibrosis transmembrane conductance regulator-derived synthetic peptide inhibits anion currents in human colonic cell line T84. J. Biol. Chem. *267*, 8411–8416.

Chao, A. C., Dix, J. A., Sellers, M. C., and Verkman, A. S. (1989). Fluorescence measurement of chloride transport in monolayer cultured cells. Mechanisms of chloride transport in fibroblasts. Biophys. J. *56*, 1071–1081.

Clarke, L. L., Grubb, B. R., Yankaskas, J. R., Cotton, C. U., McKenzie, A., and Boucher, R. C. (1994). Relationship of a non-cystic fibrosis transmembrane conductance regulator-mediated chloride conductance to organ-level disease in Cftr(-/-) mice. Proc. Natl. Acad. Sci. USA *91*, 479–483.

Cohn, J. A., Nairn, A. C., Marino, C. R., Melhus, O., and Kole, J. (1992). Characterization of the cystic fibrosis transmembrane conductance regulator in a colonocyte cell line. Proc. Natl. Acad. Sci. USA *89*, 2340–2344.

Deneka, M., Neeft, M., and van der Sluijs, P. (2003). Regulation of membrane transport by rab GTPases. Crit. Rev. Biochem. Mol. Biol. *38*, 121–142.

Denning, G. M., Ostedgaard, L. S., Cheng, S. H., Smith, A. E., and Welsh, M. J. (1992). Localization of cystic fibrosis transmembrane conductance regulator in chloride secretory epithelia. J. Clin. Invest. *89*, 339–349.

Dharmsathaphorn, K., McRoberts, J. A., Mandel, K. G., Tisdale, L. D., and Masui, H. (1984). A human colonic tumor cell line that maintains vectorial electrolyte transport. Am. J. Physiol. *246*, G204–G208.

Duman, J. G., Tyagarajan, K., Kolsi, M. S., Moore, H. P., and Forte, J. G. (1999). Expression of rab11a N124I in gastric parietal cells inhibits stimulatory recruitment of the H^+-K^+ ATPase. Am. J. Physiol. *277*, C361–372.

Elferink, L. A., and Strick, D. J. (2005). Functional properties of rab15 effector protein in endocytic recycling. Methods Enzymol. *403*, 732–743.

Gentzsch, M., Chang, X. B., Cui, L., Wu, Y., Ozols, V. V., Choudhury, A., Pagano, R. E., and Riordan, J. R. (2004). Endocytic trafficking routes of wild-type and ΔF508 CFTR. Mol. Biol. Cell.

Goldenring, J. R., Smith, J., Vaughan, H. D., Cameron, P., Hawkins, W., and Navarre, J. (1996). Rab11 is an apically located small GTP-binding protein in epithelial tissues. Am. J. Physiol. *270*, G515–G525.

Goldenring, J. R., Soroka, C. J., Shen, K. R., Tang, L. H., Rodriguez, W., Vaughan, H. D., Stoch, S. A., and Modlin, I. M. (1994). Enrichment of rab11, a small GTP-binding protein, in gastric parietal cells. Am. J. Physiol. *267*, G187–G194.

Gorvel, J. P., Chavrier, P., Zerial, M., and Gruenberg, J. (1991). rab5 controls early endosome fusion in vitro. Cell *64*, 915–925.

Guggino, W. B., and Stanton, B. A. (2006). New insights into cystic fibrosis: molecular switches that regulate CFTR. Nat. Rev. Mol. Cell Biol. *7*, 426–436.

Hallows, K. R., Kobinger, G. P., Wilson, J. M., Witters, L. A., and Foskett, J. K. (2003). Physiological modulation of CFTR activity by AMP-activated protein kinase in polarized T84 cells. Am. J. Physiol. Cell Physiol. *284*, C1297–C1308.

Howard, M., DuVall, M. D., Devor, D. C., Dong, J. Y., Henze, K., and Frizzell, R. A. (1995). Epitope tagging permits cell surface detection of functional CFTR. Am. J. Physiol. *269*, C1565–C1576.

Junutula, J. R., Schonteich, E., Wilson, G. M., Peden, A. A., Scheller, R. H., and Prekeris, R. (2004). Molecular characterization of Rab11 interactions with members of the family of Rab11-interacting proteins. J. Biol. Chem. *279*, 33430–33437.

Khvotchev, M. V., Ren, M., Takamori, S., Jahn, R., and Sudhof, T. C. (2003). Divergent functions of neuronal Rab11b in Ca2+-regulated versus constitutive exocytosis. J. Neurosci. *23*, 10531–10539.

Lai, F., Stubbs, L., and Artzt, K. (1994). Molecular analysis of mouse Rab11b: a new type of mammalian YPT/Rab protein. Genomics *22*, 610–616.

Lapierre, L. A., Dorn, M. C., Zimmerman, C. F., Navarre, J., Burnette, J. O., and Goldenring, J. R. (2003). Rab11b resides in a vesicular compartment distinct from Rab11a in parietal cells and other epithelial cells. Exp. Cell Res. *290*, 322–331.

Lapierre, L. A., Kumar, R., Hales, C. M., Navarre, J., Bhartur, S. G., Burnette, J. O., Provance, D. W., Jr., Mercer, J. A., Bahler, M., and Goldenring, J. R. (2001). Myosin vb is associated with plasma membrane recycling systems. Mol. Biol. Cell *12*, 1843–1857.

Leung, S. M., Ruiz, W. G., and Apodaca, G. (2000). Sorting of membrane and fluid at the apical pole of polarized Madin-Darby canine kidney cells. Mol. Biol. Cell *11*, 2131–2150.

Mandel, K. G., Dharmsathaphorn, K., and McRoberts, J. A. (1986). Characterization of a cyclic AMP-activated Cl-transport pathway in the apical membrane of a human colonic epithelial cell line. J. Biol. Chem. *261*, 704–712.

Opdam, F. J., Kamps, G., Croes, H., van Bokhoven, H., Ginsel, L. A., and Fransen, J. A. (2000). Expression of Rab small GTPases in epithelial Caco-2 cells: Rab21 is an apically located GTP-binding protein in polarised intestinal epithelial cells. Eur. J. Cell Biol. *79*, 308–316.

Prince, L. S., Tousson, A., and Marchase, R. B. (1993). Cell surface labeling of CFTR in T84 cells. Am. J. Physiol. *264*, C491–C498.

Prince, L. S., Workman, R. B., Jr., and Marchase, R. B. (1994). Rapid endocytosis of the cystic fibrosis transmembrane conductance regulator chloride channel. Proc. Natl. Acad. Sci. USA *91*, 5192–5196.

Rogers, C. S., *et al.* (2008). Disruption of the CFTR gene produces a model of cystic fibrosis in newborn pigs. Science *321*, 1837–1841.

Sakurada, K., *et al.* (1991). Molecular cloning and characterization of a ras p21-like GTP-binding protein (24KG) from rat liver. Biochem. Biophys. Res. Commun. *177*, 1224–1232.

Scapin, S. M., Carneiro, F. R., Alves, A. C., Medrano, F. J., Guimaraes, B. G., and Zanchin, N. I. (2006). The crystal structure of the small GTPase Rab11b reveals critical differences relative to the Rab11a isoform. J. Struct. Biol. *154*, 260–268.

Schlierf, B., Fey, G. H., Hauber, J., Hocke, G. M., and Rosorius, O. (2000). Rab11b is essential for recycling of transferrin to the plasma membrane. Exp. Cell Res. *259*, 257–265.

Simpson, J. C., Griffiths, G., Wessling-Resnick, M., Fransen, J. A., Bennett, H., and Jones, A. T. (2004). A role for the small GTPase Rab21 in the early endocytic pathway. J. Cell Sci. *117*, 6297–6311.

Sonnichsen, B., De Renzis, S., Nielsen, E., Rietdorf, J., and Zerial, M. (2000). Distinct membrane domains on endosomes in the recycling pathway visualized by multicolor imaging of Rab4, Rab5, and Rab11. J. Cell Biol. *149*, 901–914.

Swiatecka-Urban, A., Boyd, C., Coutermarsh, B., Karlson, K. H., Barnaby, R., Aschenbrenner, L., Langford, G. M., Hasson, T., and Stanton, B. A. (2004). Myosin VI regulates endocytosis of the cystic fibrosis transmembrane conductance regulator. J. Biol. Chem. *279*, 38025–38031.

Swiatecka-Urban, A., *et al.* (2005). The short apical membrane half-life of rescued ΔF508-CFTR results from accelerated endocytosis ΔF508-CFTR in polarized human airway epithelial cells. J. Biol. Chem. *280*, 36762–36772.

Swiatecka-Urban, A., *et al.* (2007). Myosin Vb is required for trafficking of the cystic fibrosis transmembrane conductance regulator in Rab11a-specific apical recycling endosomes in polarized human airway epithelial cells. J. Biol. Chem. *282*, 23725–23736.

Tousson, A., Fuller, C. M., and Benos, D. J. (1996). Apical recruitment of CFTR in T-84 cells is dependent on cAMP and microtubules but not Ca^{2+} or microfilaments. J. Cell Sci. *109*(Pt 6), 1325–1334.

Trischler, M., Stoorvogel, W., and Ullrich, O. (1999). Biochemical analysis of distinct Rab5- and Rab11-positive endosomes along the transferrin pathway. J. Cell Sci. *112*(Pt 24), 4773–4783.

Tuma, P. L., Nyasae, L. K., and Hubbard, A. L. (2002). Nonpolarized cells selectively sort apical proteins from cell surface to a novel compartment, but lack apical retention mechanisms. Mol. Biol. Cell *13*, 3400–3415.

Ullrich, O., Reinsch, S., Urbe, S., Zerial, M., and Parton, R. G. (1996). Rab11 regulates recycling through the pericentriolar recycling endosome. J. Cell Biol. *135*, 913–924.

Uzan-Gafsou, S., Bausinger, H., Proamer, F., Monier, S., Lipsker, D., Cazenave, J. P., Goud, B., de la Salle, H., Hanau, D., and Salamero, J. (2007). Rab11A controls the biogenesis of Birbeck granules by regulating Langerin recycling and stability. Mol. Biol. Cell *18*, 3169–3179.

Varga, K., *et al.* (2004). Efficient intracellular processing of the endogenous cystic fibrosis transmembrane conductance regulator in epithelial cell lines. J. Biol. Chem. *279*, 22578–22584.

Wagner, J. A., McDonald, T. V., Nghiem, P. T., Lowe, A. W., Schulman, H., Gruenert, D. C., Stryer, L., and Gardner, P. (1992). Antisense oligodeoxynucleotides to the cystic fibrosis transmembrane conductance regulator inhibit cAMP-activated but not calcium-activated chloride currents. Proc. Natl. Acad. Sci. USA *89*, 6785–6789.

Wakabayashi, Y., Lippincott-Schwartz, J., and Arias, I. M. (2004). Intracellular trafficking of bile salt export pump (ABCB11) in polarized hepatic cells: constitutive cycling between the canalicular membrane and rab11-positive endosomes. Mol. Biol. Cell *15*, 3485–3496.

Wang, X., Kumar, R., Navarre, J., Casanova, J. E., and Goldenring, J. R. (2000). Regulation of vesicle trafficking in madin-darby canine kidney cells by Rab11a and Rab25. J. Biol. Chem. *275*, 29138–29146.

Webster, P., Vanacore, L., Nairn, A. C., and Marino, C. R. (1994). Subcellular localization of CFTR to endosomes in a ductal epithelium. Am. J. Physiol. *267*, C340–C348.

Weixel, K. M., and Bradbury, N. A. (2000). The carboxyl terminus of the cystic fibrosis transmembrane conductance regulator binds to AP-2 clathrin adaptors. J. Biol. Chem. *275*, 3655–3660.

Yang, Y., Devor, D. C., Engelhardt, J. F., Ernst, S. A., Strong, T. V., Collins, F. S., Cohn, J. A., Frizzell, R. A., and Wilson, J. M. (1993). Molecular basis of defective anion transport in L cells expressing recombinant forms of CFTR. Hum. Mol. Genet. *2*, 1253–1261.

Zeitlin, P. L., *et al.* (1992). CFTR protein expression in primary and cultured epithelia. Proc. Natl. Acad. Sci. USA. *89*, 344–347.

Zerial, M., and McBride, H. (2001). Rab proteins as membrane organizers. Nat. Rev. Mol. Cell Biol. *2*, 107–117.